

# UNCLASSIFIED

AD NUMBER
AD803070
NEW LIMITATION CHANGE
TO Approved for public release, distribution unlimited
FROM Distribution authorized to U.S. Gov't. agencies and their contractors; Critical Technology; OCT 1966. Other requests shall be referred to Air Force Materials Lab., Wright-Patterson AFB, OH 45433.
AUTHORITY
AFML ltr, 7 Dec 1972

THIS PAGE IS UNCLASSIFIED

AFML-TR-66-343

DEVELOPMENT OF HYDROTHERMAL METHOD FOR  
GROWING LARGE, HIGH PURITY SINGLE CRYSTALS OF BERYLLIUM  
OXIDE, AND INITIATE RESEARCH ON GROWING SINGLE CRYSTALS  
OF 'KTN' AND CHRYSOBERYL

V. G. Hill and R. L. Harker  
Tem-Pres Research, Inc.

TECHNICAL REPORT NO. AFML-TR-66-343

October 1966

This document is subject to special export controls and each transmittal to foreign governments or foreign nationals may be made only with prior approval of the Air Force Materials Laboratory (MAYT), Wright-Patterson Air Force Base, Ohio 45433.

Air Force Materials Laboratory  
Research and Technology Division  
Air Force Systems Command  
Wright-Patterson Air Force Base, Ohio

803070

## NOTICES

When Government drawings, specifications, or other data are used for any purpose other than in connection with a definitely related Government procurement operation, the United States Government thereby incurs no responsibility nor any obligation whatsoever; and the fact that the Government may have formulated, furnished, or in any way supplied the said drawings, specifications, or other data, is not to be regarded by implication or otherwise as in any manner licensing the holder or any other person or corporation, or conveying any rights or permission to manufacture, use, or sell any patented invention that may in any way be related thereto.

Copies of this report should not be returned to the Research and Technology Division unless return is required by security considerations, contractual obligations, or notice on a specific document.

AFML-TR-66-343

DEVELOPMENT OF HYDROTHERMAL METHOD FOR  
GROWING LARGE, HIGH PURITY SINGLE CRYSTALS OF BERYLLIUM  
OXIDE, AND INITIATE RESEARCH ON GROWING SINGLE CRYSTALS  
OF 'KTN' AND CHRYSOBERYL

V. G. Hill and R. I. Harker  
Tem-Pres Research, Inc.

TECHNICAL REPORT NO. AFML-TR-66-343

October 1966

This document is subject to special export controls and each transmittal to foreign governments or foreign nationals may be made only with prior approval of the Air Force Materials Laboratory (MAYT), Wright-Patterson Air Force Base, Ohio 45433.

Air Force Materials Laboratory  
Research and Technology Division  
Air Force Systems Command  
Wright-Patterson Air Force Base, Ohio

## FOREWORD

This report was prepared by Tem-Pres Research, Inc., State College, Pennsylvania, under Contract AF 33(615)-1712. The contract was initiated under Project No. 7371, "Applied Research in Electrical, Electronic, and Magnetic Materials", Task No. 737101, "Dielectric and Related Materials." The work was administered under the direction of the Air Force Materials Laboratory, Research and Technology Division, Air Force Systems Command, Wright-Patterson Air Force Base, Ohio, with Mr. Robert L. Hickmott and Paul W. Dimiduk as project engineers.

This report covers work conducted from 1 September 1965 to 31 August 1966.

The manuscript was released by the authors in September 1966 for publication as an RTD Technical Report.

The report is presented in three chapters, each covering the research on a particular compound. Chapter 1 deals with Beryllium oxide, Chapter 2 with  $\text{KTa}_{0.65}\text{Nb}_{0.35}\text{O}_3$  (KTN), and Chapter 3 with Chrysoberyl.

This technical report has been reviewed and is approved.



HYMAN MARCUS, Actg. Chief  
Thermo & Chemical Physics Branch  
Materials Physics Division  
Air Materials Laboratory

## ABSTRACT

Beryllium oxide crystals weighing up to 1.07 grams have been grown hydrothermally with the nutrient temperature at  $535 \pm 5^\circ\text{C}$  and the growth temperature at  $505 \pm 5^\circ\text{C}$ . Four normal potassium hydroxide was used as hydrothermal solution. Growth occurred in the vapor phase above the potassium hydroxide solution. The quality of the seeds used has a major effect on the quality of the crystals grown. The relative growth rates in the various directions are:

$$[11.0] > [00.1] \approx [00.\bar{1}] > [11.1] > [10.1] > [10.0]$$

It is the positive pyramidal termination which is nucleated and grows on the seed. The crystals grown have been characterized by chemical, petrographic, and x-ray diffraction methods, and one crystal in particular has been shown to be of high quality. Growth rate measurements of BeO are reported.

An exsolution dome has been found in the system  $\text{KNbO}_3\text{-KTaO}_3$ , and the composition  $\text{KTa}_{0.85}\text{Nb}_{0.15}\text{O}_3$  (KTN), which has useful electro-optical properties at room temperatures, is metastable at temperatures below  $900 \pm 10^\circ\text{C}$ . The hydrothermal growth of KTN single crystals is, therefore, not feasible with the equipment currently available.

Solubility determinations of chrysoberyl have been made in KOH, NaOH and water. The values obtained are far greater than those of either  $\text{Al}_2\text{O}_3$  or BeO.

## TABLE OF CONTENTS

	PAGE
CHAPTER 1. BERYLLIUM OXIDE	1
I. INTRODUCTION	1
II. PREVIOUS WORK	2
III. EQUIPMENT AND MATERIALS	5
Hydrothermal Equipment	5
Starting Materials	5
Crystal Characterization Equipment	7
IV. CULTURE AND PREPARATION OF SEEDS	8
Culture of Seeds	8
Orientation and Cutting of Seeds	8
Internal Assembly in Autoclave	11
V. RESULTS	16
Growth Rate Measurements	16
Effects of Impurities on the Crystal	22
Characterization of Crystals	24
VI. DISCUSSION OF RESULTS	32
VII. CONCLUSIONS	34
VIII. FUTURE WORK	35
IX. REFERENCES	36
CHAPTER 2. POTASSIUM TANTALATE-NIOBATE (KTN), $\text{KTa}_{0.65}\text{Nb}_{0.35}\text{O}_3$	37
I. INTRODUCTION	37
II. PREVIOUS WORK	39
III. APPROACH	40
IV. EXPERIMENTAL	41
Starting Materials	41
Equipment and Techniques	41
Subsolidus Phase Relations in the System $\text{KNbO}_3\text{-KTaO}_3$	41
Compositional Variations in Crystals	43

## TABLE OF CONTENTS

V.	DISCUSSION OF RESULTS	47
VI.	CONCLUSIONS	48
VII.	REFERENCES	49
CHAPTER 3.	CHRYSOBERYL	50
I.	INTRODUCTION	50
II.	PREVIOUS WORK	51
III.	EXPERIMENTAL	52
	Equipment	52
	Starting Materials	52
	Procedures	52
	Results	52
IV.	DISCUSSION OF RESULTS	54
V.	REFERENCES	56
	APPENDIX 1	57
	APPENDIX 2	63



## LIST OF ILLUSTRATIONS

FIGURE NO.	TITLE	PAGE
1	Phase Relationships in the Systems BeO-H <sub>2</sub> O	3
2	Solubility Curves of BeO in 4N-KOH Solution at 1,000 and 4,000 Bars as a Function of Temperature	4
3	Tem-Pres Gradient Furnaces with Independent Zone Controllers for LRA-150 Type Autoclaves	6
4	Diagram Indicating the Pertinent Axes for the Orientation of a BeO Crystal for the (11.1) Face Using the (10.0) and (10.1) Faces	10
5	Location of the Various Seed Plates Which Have Been Studied in the Hydrothermal Growth of BeO Crystals	13
6	BeO Seeds Suspended from Lower Silver Washer	14
7	BeO Seeds Suspended on Platinum Ladder Assembly	14
8	Baffle and Nutrient Basket Assemblies	15
9	Photomicrographs of [00.1] Sections through BeO Crystals Grown on [00.1] Seed Plates	18
10	High Quality BeO Crystals	19
11	Ladder Assembly with Grown BeO Crystals at the End of Run	20
12	BeO Crystals Grown on [00.1] Seed Plates	21
13	Optical Photographs of (10.1) Face of Crystal, Figure 10 (see page 19)	27
14	Berg-Barrett Photograph of (10.1) Face of Crystal 1, Figure 10 (see Figure 13)	28
15	Optical Photograph of (10.0) Face of Crystal 2, Figure 10	29
16	Optical Photograph of Adjacent (10.0) Face of Crystal 2, Figure 10	30
17	Berg-Barrett Photograph of (10.0) Face of Crystal 2, Figure 10	31
18	Berg-Barrett Photograph of Part of Figure 17 Enlarged	31

# ILLUSTRATIONS

FIGURE NO.	TITLE	PAGE
19	Transition Temperatures and $T_{CB}$ as a Function of Composition in $\text{KNbO}_3\text{-KTaO}_3$ Solid Solution	38
20	Phase Diagram for the System $\text{KNbO}_3\text{-KTaO}_3$	38
21	Subsolidus Equilibrium Phase Relations in the System $\text{KNbO}_3\text{-KTaO}_3$	42
22	Largest KTN ( $\text{KTa}_{.75}\text{Nb}_{.25}\text{O}_3$ ) Crystals Grown Hydrothermally	44
23	Exsolution Pattern in KTN Crystal Grown in Run 924 - Polarized Light	45
24	Exsolution Pattern in KTN Crystals Grown in Run 924 - Crossed Nicols	45
25	Solubility of Chrysoberyl in Potassium Hydroxide Solutions and Water vs. Temperature at Selected Pressures	53
26	Solubility of Chrysoberyl in Potassium Hydroxide Solutions vs. Normality at Selected Temperatures, and Pressures up to 4,000 Bars	55
27	LRA-150 Pressure Vessel Assembly	63

# TABLES

TABLE NO.	TITLE	PAGE
1	Semi-Quantitative Spectrographic Analyses of BeO Starting Materials	5
2	Interplanar Angles for BeO	9
3	X-Ray Reflections for Checking Orientation of BeO Crystals	12
4	Growth Rate Measurements of BeO Crystals in 4N-KOH	17
5	Semi-Quantitative Spectrochemical Analyses of BeO Crystals	25
6	Effects of Seed Quality on Overgrowth	32
7	Summary of Hydrothermal Runs in System $\text{KNbO}_3\text{-KTaO}_3$	57
8	Summary of Dry Runs in the System $\text{KNbO}_3\text{-KTaO}_3$	61
9	Solubility Determinations of Chrysoberyl	62

## CHAPTER I. BERYLLIUM OXIDE

### I. INTRODUCTION

Beryllium oxide has recently attracted special attention as a ceramic material, because in comparison to alumina it has a very high melting point, comparable mechanical strength, lower specific gravity, higher electrical resistance particularly at elevated temperatures, and an incomparably greater thermal conductivity. These properties, particularly the latter two, make it unique for heat sink applications in electronic devices. The fabrication of devices from single crystals rather than from pressed polycrystalline aggregates is desirable because it is then possible to specify the required tolerances to a very high degree of precision. This is particularly important where weight, size and the reliability of the component are important factors in the design of the device. Also there is a higher probability for epitaxial growth on single crystal substrates.

The objective of this research project is the growth of large high quality BeO crystals. This program was divided into three steps: (a) the growth of seed material of satisfactory quality, (b) the determination of the optimum conditions for the transport of materials from the nutrient zone to the seeds, and (c) the growth of high quality crystals. The work done during the first year was concerned with the first two steps, and it was conducted on a very small scale. During the first half of this year, we were particularly concerned with scaling up the equipment and making it operate under the conditions previously determined, so that larger crystals could be grown. In the latter half of the year, we were interested in refining the optimum conditions for growing large crystals and the growth and characterization of these crystals.

The two difficulties encountered have been firstly, the initial growth of crystals of satisfactory quality and size so that slices of different orientations can be made for the study of their overgrowth characteristics, and secondly, the prevention of the incorporation of impurities, including silver, into the crystals.

The crystallographic orientation of the seed used for growing a crystal is one of the most important factors affecting the growth, because it has a direct bearing on both the growth rate and quality of the crystal produced. This is well illustrated by the growth of quartz<sup>(1)</sup>. The successful growth of BeO crystals is complicated by the (00.1) plane being a twin plane.

A complementary program on the characterization of the crystals grown was initiated along with the growth program. This work included not only considerations of the chemical purity of the crystals produced, but also their crystallographic perfection.

## II. PREVIOUS WORK

Most of the previous attempts to grow BeO crystals involved either crystallization from molten salts or vapor phase techniques<sup>(2, 3, 4)</sup>. Newkirk and Smith<sup>(4)</sup> investigated the application of hydrothermal methods to the growth of BeO crystals in neutral and alkaline environments, and Newkirk<sup>(5)</sup> determined the stability relations in the systems BeO-H<sub>2</sub>O, and Na<sub>2</sub>O-BeO-H<sub>2</sub>O at concentrations of NaOH solutions to 8.02 molal, as a function of temperature and pressure up to 600°C, and 4,100 bars. No noticeable difference was found between the phase diagram for the former (Figure 1), and that with NaOH solutions. He found that the univariant reaction curve passed through the points 200°C at 4,100 bars, and 170°C at 300 bars. He also observed that BeO formed in the range 175 to 250°C was not well developed, and possessed a larger unit cell than that attributed to BeO. Newkirk and Smith demonstrated that small BeO crystals could be grown hydrothermally in 2.03 M-NaOH solutions at 400°-425°C and 2,000 bars. They obtained prismatic crystals 0.125 inch long, and which grew in the positive polar direction at a rate of 0.005 inch per day. Hill and Harker<sup>(6)</sup> showed that 4N-KOH solution was perhaps a superior solvent producing crystals of high quality. They determined the solubility curve of BeO in this and other solvents at 1,000 and 4,000 bars. (Figure 2). The former curve is interesting in that it is composed of two separate parts a low temperature region where the slope of the curve is slight and a higher temperature region where there is a significantly greater slope to the curve. This information offered the possibility of controlling growth rate very precisely. Slow growth could be achieved by working in the lower temperature region while a faster rate was possible by working in the high temperature region. Growth control may also be exercised by working at pressures between 1,000 and 4,000 bars. The last possibility is attractive, but has the disadvantage that there is a drop in solubility as pressure is increased. This could result in poor overgrowth because of the rapid increase in growth rate while the pressure is being increased.

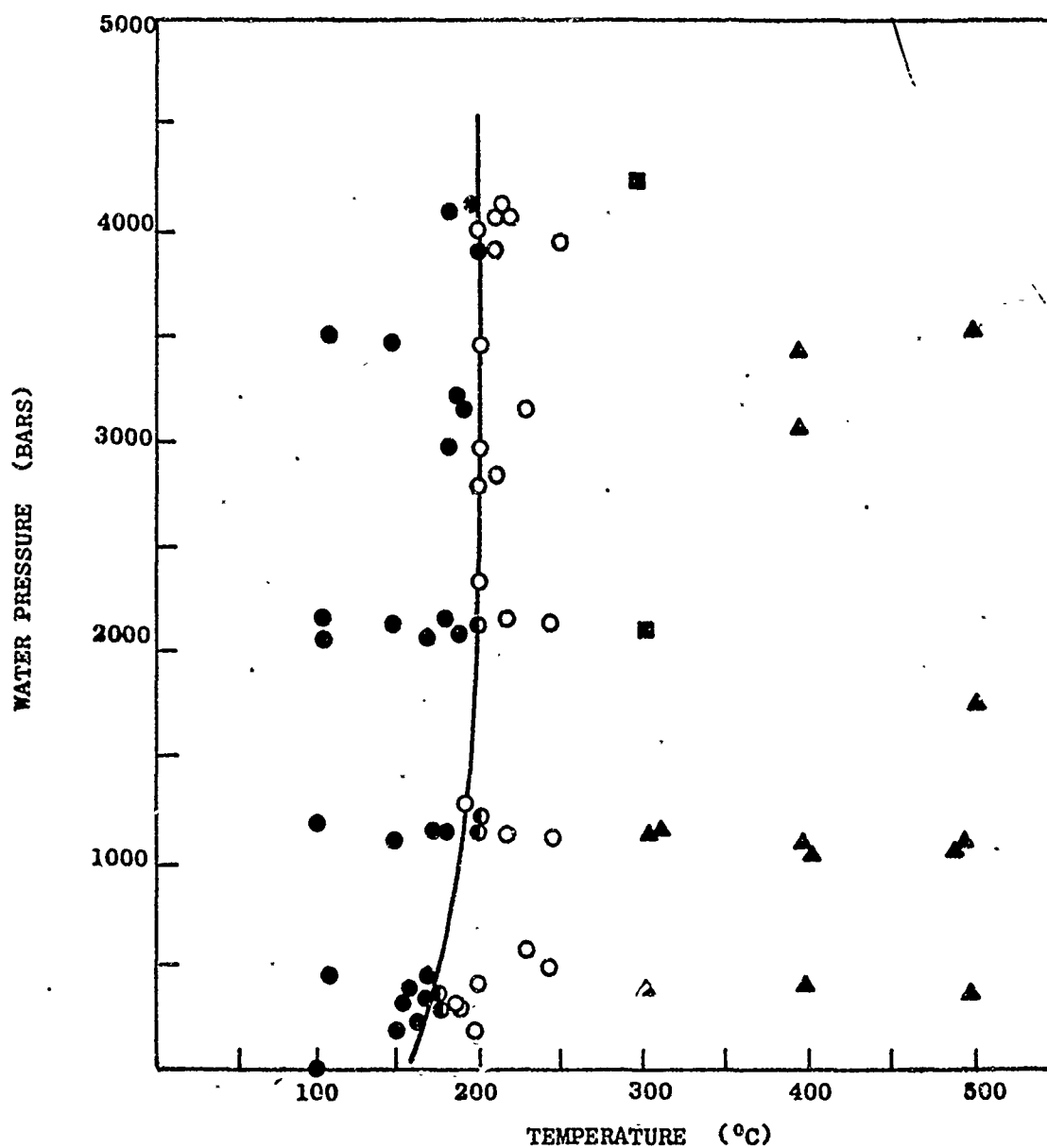


Figure 1. Phase Relationships in the System  $\text{BeO-H}_2\text{O}^{(5)}$

Berylco and  $\beta\text{-Be(OH)}_2$  used as the starting materials. Filled circles  $\beta\text{-Be(OH)}_2$ . Squares: BeO. Triangles: well crystallized BeO. Open circles: BeO with enlarged unit cell. Half-filled circles: BeO with enlarged unit cell and  $\beta\text{-Be(OH)}_2$ .

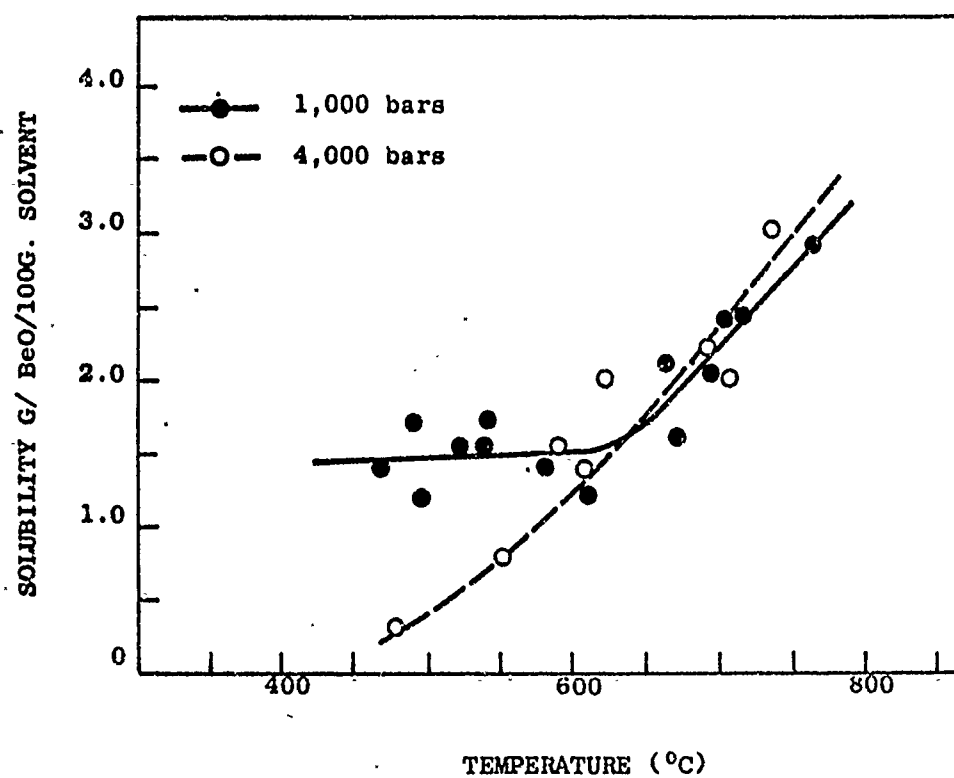


Figure 2. Solubility Curves of BeO in 4N-KOH Solution at 1,000 and 4,000 bars as a Function of Temperature (6).

### III. EQUIPMENT AND MATERIALS

#### Hydrothermal Equipment

Three hydrothermal crystal growing systems are available for this work. These were designed to take the Tem-Pres LRA-150 series of autoclaves. The furnaces are Kanthal wound and have two independently controlled temperature zones. Two of these (Figure 3) have variacs between the control system and the furnace so that the furnace power can be varied to give better control of the temperature gradient in the furnace. The third system incorporates saturable core reactors between the controllers and the furnace. This is particularly useful when small thermal gradients are required.

The autoclaves used are the LRA-150\* series fabricated of René alloy, and Haynes Stellite Alloy No. 25. The interior of the vessel is lined with a closely fitting silver thimble. The internal dimensions of the vessels are 1.25 inches diameter and 7.0 inches deep. The seal is of the modified Bridgman type, with one silver and one brass washer. This has the advantage of producing a good seal with little distortion of the washer. This is particularly important at temperatures above 500°C, because of the plastic flow of silver above this temperature and at the pressures involved.

#### Starting Materials.

The manufacturers hatch analysis of the BeO powder used was 99.9%, and the KOH 99.9+%, these were both supplied by the Gallard-Schlesinger Chemical Mfg. Corporation, Carle Place, L.I., N. Y. Demineralized water from a mixed bed unit was used to prepare solutions. The BeO powder was formed into pellets and fired to about 1400°C by Coors Porcelain Company, Golden, Colorado. The spectrographic analysis of the BeO powder and the pellets made from it are given in Table I.

TABLE I

#### SEMI-QUANTITATIVE SPECTROGRAPHIC ANALYSIS OF BeO STARTING MATERIALS

Element	Powder	Pellets
Ca	2 ppm	1000 - 40 ppm
Al	20	1000 - 300
Si	100	1000
Ag	< 2	< 2 - not detected
Mg	< 5	1000 - 300
Ti	10	20 - 10
Na	< 10	< 10
K	< 10	< 10

\*Sought but not detected: Sr, Ba, Cr, B, Mn, Sb, Zn, Pb, Ge, Co, Zr, Bi, V, Ni, Li, and Cd. (Mr. N. H. Suhr, analyst.)





Figure 3. Tem-Pres Gradient Furnaces, With Independent Zone Controllers for LRA-150 Type Autoclaves.

The semi-quantitative spectrochemical analyses show that the pellets were contaminated at some stage in the fabrication process. The contamination was, however, not homogeneous because quite different results were obtained between the values of replicate analyses of two samples from the batch of pellets. It will be shown later that of the contaminants, only  $\text{SiO}_2$  is significant as far as the growing crystal is concerned.

#### Crystal Characterization Equipment

A General Electric x-ray diffractometer with copper radiation was used to record the diffraction peaks from the various faces of the  $\text{BeO}$  single crystals. The diffractometer was equipped with a goniostat for alignment of the crystals.

X-ray topography was done using similar equipment to that described by Webb<sup>(7)</sup>.

#### IV. CULTURE AND PREPARATION OF SEEDS

##### Culture of Seeds

Large high quality crystals of bromellite ( $\text{BeO}$ ) are not known to occur in nature and so much effort was spent on the culture of seeds. This is necessary because it is usual for the quality of the overgrowth to be poorer than that of the initial seed, and the size of the seed used has a direct bearing on the size of the crystal grown.

Small seeds 0.1 and 0.2 inch were obtained from the walls of the LRA-150 vessels in most crystal growth runs. However, because of the mutual interference of the crystals their quality decreased with size, and therefore with the duration of the runs. This was particularly evident at high temperatures. A 0.013 inch diameter hole was drilled through the better crystals and a 0.01 inch diameter platinum wire threaded through. These crystals were then suspended in 5 or 10 mm diameter gold tubes. Four normal KOH solution was used as solvent and pelletized  $\text{BeO}$  as nutrient. These over-grown crystals were further examined and the best ones selected for further overgrowth. These were later used for growth studies, and when they were large enough  $[00.1]$  plates were cut from them with a sonic cutter. In a few cases, the pyramidal terminations and  $[10.1]$  oriented slices were used as seeds. It was only in the later stages of the work that seeds of other orientations could be cut, because the larger crystals which were grown usually contained only a small area of sufficiently high quality suitable for the cutting of seeds.

It was necessary in all cases to determine the quality of the seeds to be used in each run. To do this the opposite faces of the seeds were polished. These were then examined under the binocular and petrographic microscopes. Both reflected and transmitted light were used. Particular attention was paid to the presence of twinning, inclusions, cracks and strain. A defect which was present in most of the seeds was the ghost boundaries of each overgrowth cycle. These were not well defined when the overgrowth occurred in the lower temperature region of the solubility curve. However, where rapid growth occurred in the higher temperature region a well defined junction was observed. Often this contained a small amount of fluid. When a  $[00.1]$  plate was used as seed a series of inclusions were present. In some cases these had regular outline, but in others they were irregular. Seeds which were twinned, had major cracks, or had many inclusions were rejected.

##### Orientation and Cutting of Seeds

As the crystal growth studies progressed, seed crystals of particular crystallographic orientations were needed for the study of their growth characteristics. The procedure used was to mount the crystal, from which it was desired to cut the seeds, on a goniometer and identify a reference

face with an x-ray diffractometer. The crystal was then rotated through the correct angle necessary to bring the required plane into reflecting position, so that the angle between the reference face and the desired plane could be checked on the diffractometer. Usually the (10.0) face was used as the reference face. The [11.1] slice was the only exception to this procedure because it does not give a reflection. The slices were cut with a diamond saw having two axes of rotation to make the required adjustments.

The cell constants used in the calculation for the procedure were  $a = 2.698 \text{ \AA}$ ,  $c = 4.330 \text{ \AA}$ . The interplanar angles were calculated from the equation:

$$\cos \phi = \frac{h_1 h_2 + k_1 k_2 + 1/2(h_1 k_2 + h_2 k_1) + 3/4(a/c)^2 l_1 l_2}{\sqrt{h_1^2 + k_1^2 + h_1 k_1 + 3/4(a/c)^2 l_1^2} \cdot \sqrt{h_2^2 + k_2^2 + h_2 k_2 + 3/4(a/c)^2 l_2^2}}$$

where  $(h_1 \ k_1 \ l_1)$  and  $(h_2 \ k_2 \ l_2)$  are the indices of the planes concerned. The angles calculated between the planes in which we were interested are listed in Table 2.

TABLE 2

INTERPLANAR ANGLES FOR BeO

$h_1$	$k_1$	$l_1$	$h_2$	$k_2$	$l_2$	$\phi$
1	0	0	0	1	0	60
1	0	0	0	0	1	90
1	0	0	1	1	0	30
1	1	0	1	1	1	17.1
0	0	1	1	1	1	72.9
1	0	0	1	0	1	28.1
0	0	1	1	0	1	61.9
1	0	1	1	1	1	29.7

Since the location of the (11.1) face could not be confirmed by the x-ray diffractometer, a variation of the above procedure was used. The pertinent axes for the orientation of the crystal for the (11.1) face using the (10.0) and (10.1) faces are indicated diagrammatically in Figure 4.

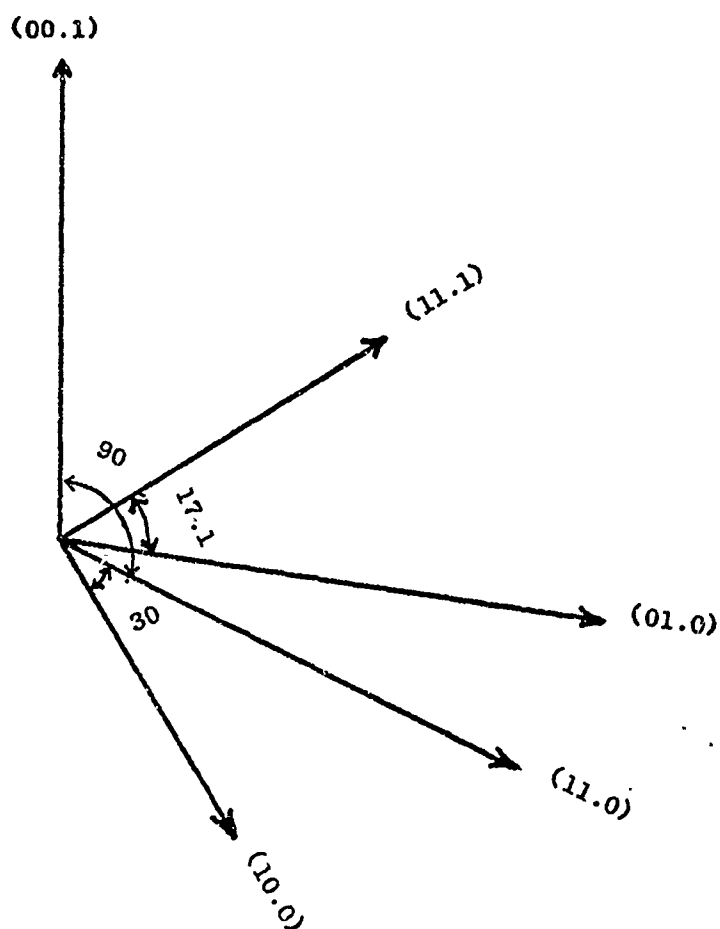


Figure 4. Diagram Indicating the Pertinent Axes for the Orientation of a BeO Crystal for the (11.1) Face Using the (10.0) and (10.1) Faces.

Table 3 lists the x-ray reflections used for checking the orientation of the planes of the crystals.

In the cutting operation the (10.0) face of the crystals was oriented parallel to the normal cutting wheel plane with the (00.1) vertical. The base of the saw was then turned  $30^\circ$  and the cutting wheel tilted  $17.1^\circ$ . The slices were then made. In all cases a 0.013 inch diameter hole was drilled through the seed plates and a 0.01 inch diameter platinum wire threaded through them, and tied. The seeds were then thoroughly cleaned by washing with xylene, then acetone and dried. After this, they were allowed to stand overnight in warm concentrated HCl, washed and dried. The seeds were then stored in a clean stoppered bottle ready for use.

The orientations used are (00.1), (10.0), (10.1), (11.1), and (11.0). Figure 5 shows the location of these planes in the crystal.

#### Internal Assembly in Autoclave

Two methods of suspending the seeds were used, (Figures 6 and 7). In the first method the suspending platinum wires were directly attached to a lower silver plate at the closure of the autoclave. The second method was the suspension of the seeds from a ladder made of platinum wire. This ladder was suspended from a lower silver washer placed below the plunger. The former method was useful where the direct comparison of the growth of a number of seeds was required. The latter method was preferred for crystal growing runs of much longer duration, because it reduced the risk of mutual interference of crystals. It was used almost exclusively during the latter part of the program.

The autoclaves were divided into two "isothermal" regions by a baffle of the type illustrated in Figure 8. The baffles had a 10 percent opening. The baffle was held in position by two silver rods joining it to a silver basket at the bottom of the vessel. This basket contained the nutrient material. The silver thimble lining the autoclave, baffle and basket assembly, and closure plate were all made from silver of the same composition (99.99% pure, suppliers specification).

TABLE 3

X-RAY REFLECTIONS FOR CHECKING ORIENTATION OF BeO CRYSTALS<sup>(1)</sup>

2 $\theta$	hkl	Rel. Intensity
38.5	1 0 0	91
41.3	0 0 2	61
43.9	1 0 1	100
57.7	1 0 2	22
69.7	1 1 0	29
77.0	1 0 3	24
82.6	2 0 0	4
84.4	1 1 2	16
86.6	2 0 1	5
89.4	0 0 4	<1
96.8	2 0 2	3
102.0	1 0 4	<1
115.2	2 0 3	10
121.4	2 1 0	4
125.9	2 1 1	5
130.0	1 1 4	2
139.9	1 0 5	14
140.7	2 2 2	8

(1) Swanson and Tatge<sup>(8)</sup>, (2 $\theta$  angles calculated for CuK $\alpha$  radiation  
= 1.5418 Å)

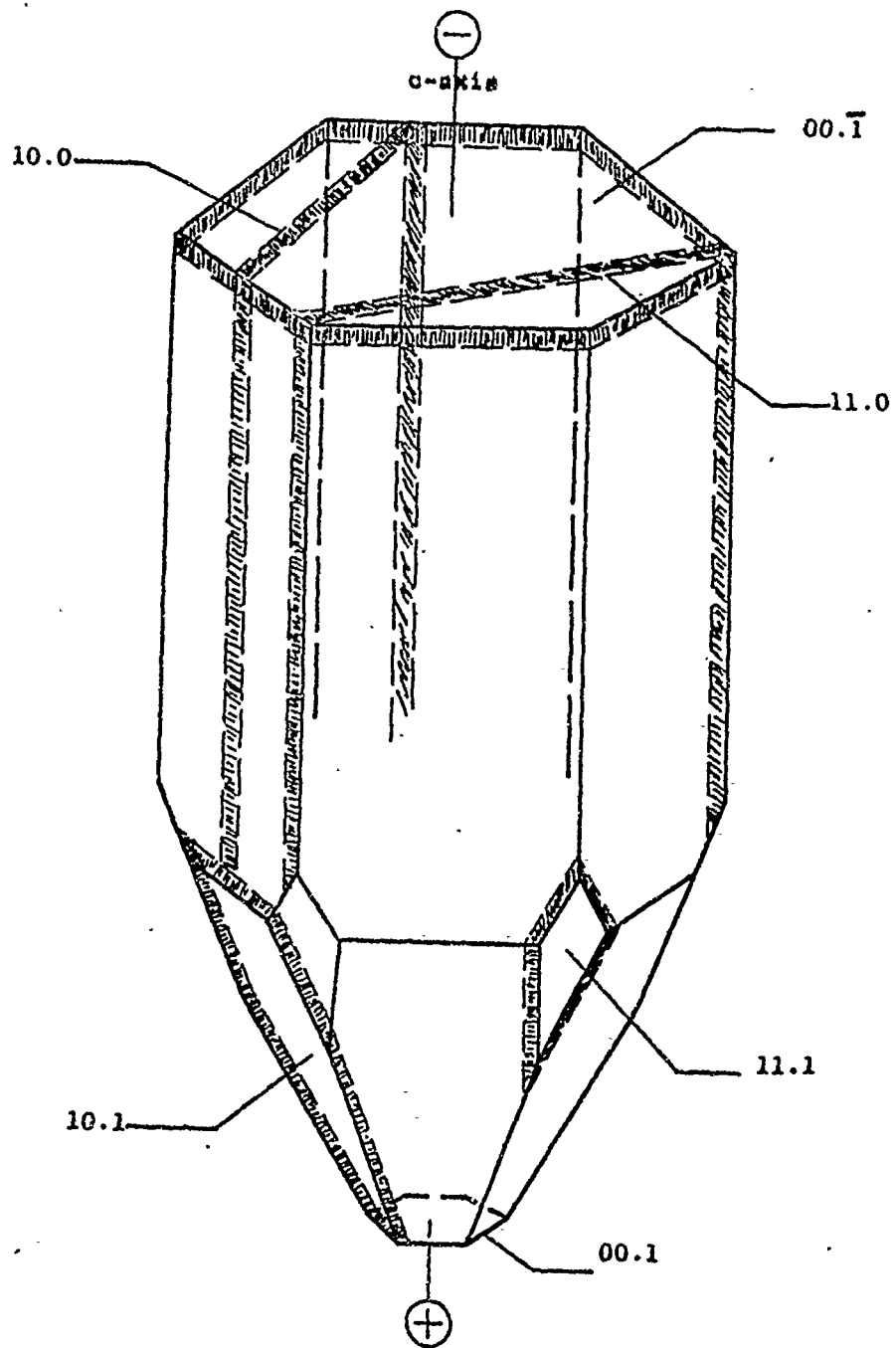


Figure 5. Location of the Various Seed Plates Which Have Been Studied in the Hydrothermal Growth of BeO Crystals.



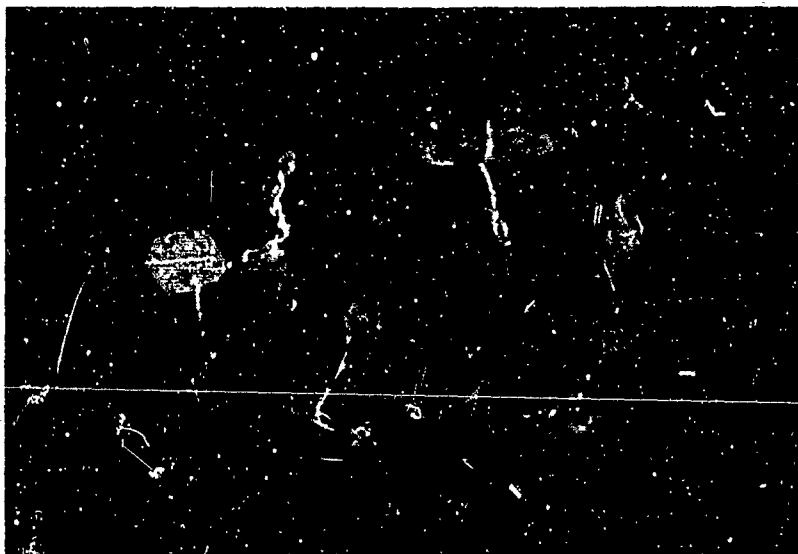


Figure 6. BeO Seeds Suspended from Lower Silver Washer. (Run 829)

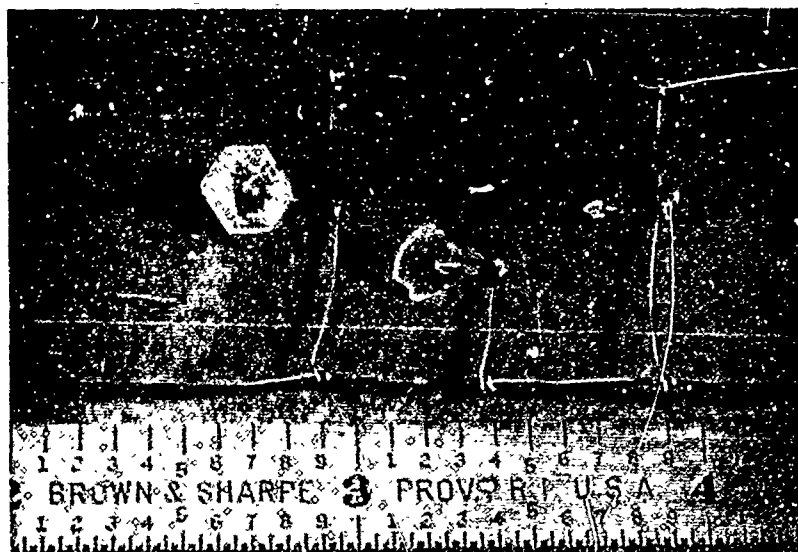


Figure 7. BeO Seeds Suspended on Platinum Ladder Assembly. (Run 919)

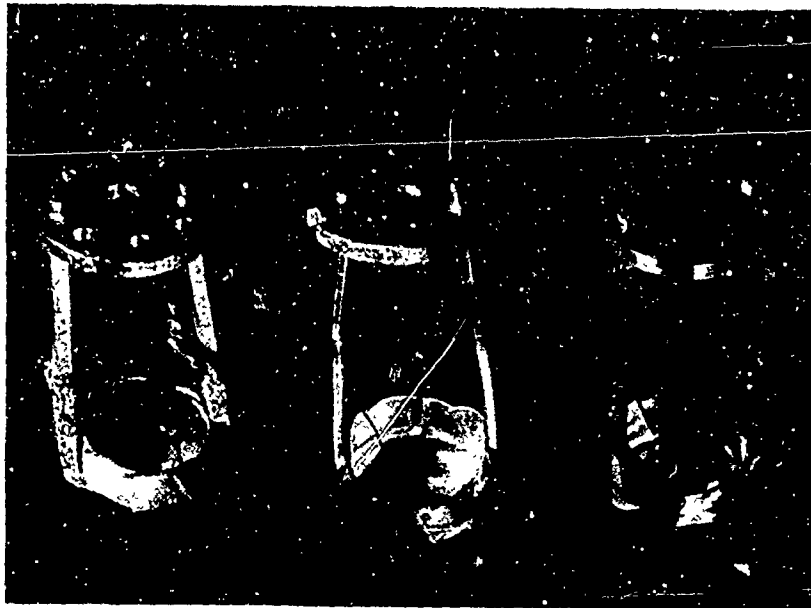


Figure 8. Baffle and Nutrient Basket Assemblies.

Note corrosion marks on the last two assemblies, which have been used, and the extensive growth of silver crystals on the last assembly. Heaviest growth is at what appears to be liquid-vapor interface - run 880.

## V. RESULTS

### Growth Rate Measurements

It was observed that the growing area was the positive pyramidal termination, and it was this that was nucleated, and subsequently generated the other faces. It was also observed that the  $(00\bar{1})$  plane acted as a twin plane. The result was that where the  $(00\bar{1})$  was exposed for growth the positive pyramids which nucleated there initially resulted in an area of poor growth. However, since all these were in the same crystallographic orientation it was possible for them to heal by lateral growth. Unfortunately, this only occurred when the growth perpendicular to the  $c$ -axis was sufficiently fast to keep pace with the growth along the  $c$ -axis. So far, this has only been checked in one run. Usually the lateral growth was so much slower and poorer in quality than that along the  $c$ -axis that a zone of inclusions occurred parallel to the  $c$ -axis.

A summary of the growth rate measurements completed to date is given in Table 4.

The presence of a poor junction between the seed and the overgrowth material has been a major factor causing the growth of poor quality crystals (Figure 9). This problem has been successfully solved by programming the heating cycle of the vessel. Three heating cycles were studied: (a) rapid heating to temperature, (b) slow heating to temperature, (c) rapid heating to a fixed temperature followed by slow heating. The first procedure gave the poorest junction of overgrowth to the seed. The second often resulted in the complete solution of the seed. In the third cycle, it was found convenient to heat the autoclave to  $400 \pm 20^\circ\text{C}$  and maintain this temperature for 24 hours. The temperature of the autoclave was then raised to the desired value over a 24 hour period, while at the same time a temperature gradient of  $10^\circ\text{C}$  was maintained between the nutrient and growth zones. The autoclave was only adjusted to the desired operating temperature when the temperature of the nutrient zone was within  $20^\circ\text{C}$  of that desired for the seed zone. This method permitted the dissolving of sufficient material from the seed for it to present a 'clean' surface for growth, and so a good junction is possible.

$\text{BeO}$  crystals of the highest quality were grown in run 920 (Figure 10). The nutrient temperature was  $527^\circ\text{C}$  and the seed temperature  $504^\circ\text{C}$ . A stepwise heating cycle was used. The crystal grown on the  $[00\bar{1}]$  seed plate was of slightly lower quality, and appeared to contain a significantly higher dislocation density than the other. Detailed evaluation of these crystals will be discussed later in this report. Some other runs have yielded even larger crystals than those illustrated in Figure 10. The largest of these obtained so far are shown in Figure 11 (Run 938). The crystal labelled (6) weighs 1.07 g., and those labelled (1) and (2) are only slightly smaller. The poorer quality of these crystals reflect the quality of the seeds used. The slices were obtained from the crystal shown in the upper left hand corner of Figure 12.

TABLE 4

## GROWTH RATE MEASUREMENTS OF BeO CRYSTALS IN 4N-KOH

Run No.	Temperature °C		Orientation	Run Duration in Days	No. of Meas.	Growth Rate ins/day	
	Nutrient	Seed				Parall. to c-axis	Perp. to c-axis
700	728	700	Prism. cryst. (1)	8	1	0.014	-
810	590	580	Prism. cryst. (2)	11	3	0.009	0.002
820	580	570	Pyrd. term. (3)	31	3	0.006	0.003
			(00.1) plate		2	0.008	0.003
			(00.1) term.		1	0.012	-
921	581	575	(10.1) plate	23	1	0.003	0.002
			(00.1) plate		1	0.003	0.0004
			Prism. cryst.		1	0.003	0.001
919	575	554	(10.1) plate	20	1	(0.002)	0.001
			(00.1) plate		1	0.005	0.001
			Prism. cryst.		1	0.007	0.001
880	571	551	(00.1) plate	37	2	0.006	0.002
657	561	530	(00.1) plate	14	5	0.005	0.001
656	548	532	(00.1) plate	14	5	0.004	0.001
833	543	533	Pyrd. term.	62	4	0.002	0.0006
838	535	502	(10.1) plate	90	1	0.0026	0.0015
			(11.1) plate		1	0.0031	0.0010
			(00.1) plate		1	0.0032	0.0002
			Pyrd. term.		1	0.0023	0.0004
			Prism. cryst.		1	0.0011	0.0003
			(11.0) plate		1	0.0037	0.0014
920	527	504	(10.1) plate	68	1	(.0015)	-
			(00.1) plate		1	(.0001)	(0.0001)
			Prism. cryst.			0.001	.0001

(1) Prismatic crystal with positive pyramidal termination

(2) Positive pyramidal termination of crystal

(3) Plate of the orientation indicated sawn from the crystal

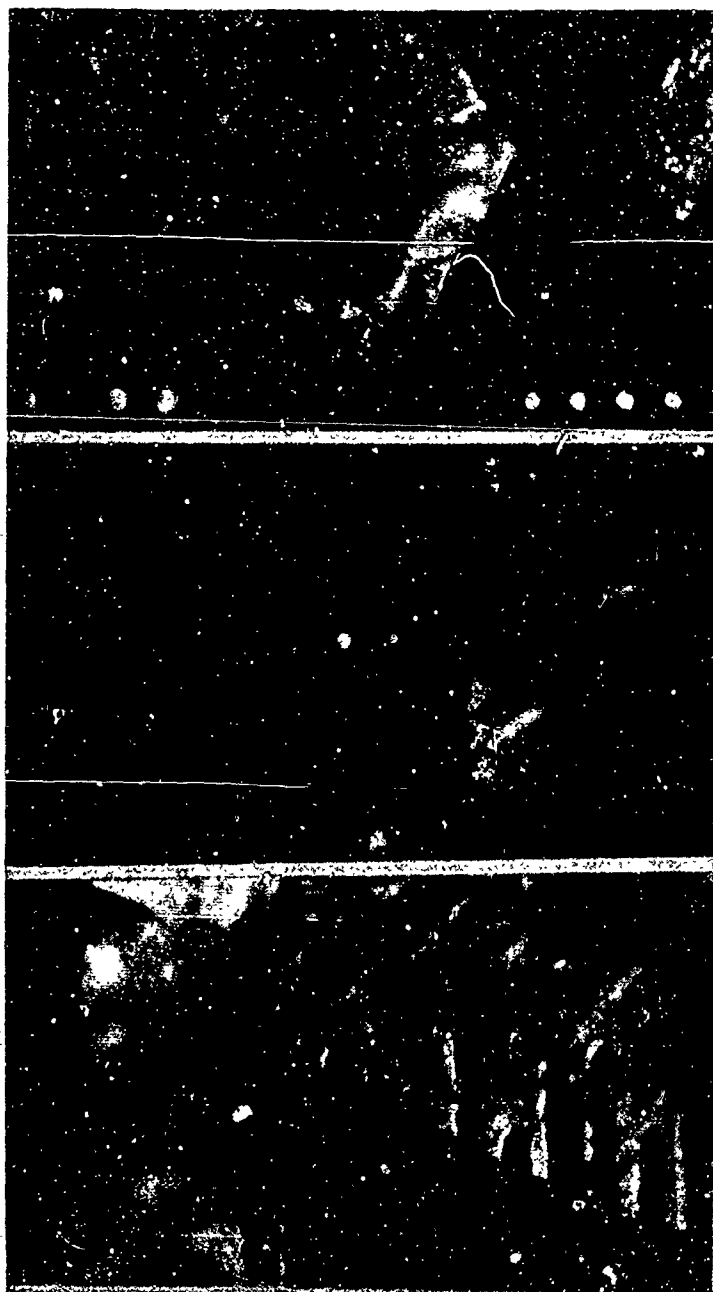


Figure 9. Photomicrographs of  $[00.1]$  Sections Through BeO Crystals Grown on  $[00.1]$  Seed Plates. (Run 829)

Note varying sharpness of junction of overgrowth material with  $(10.0)$  face. Small divisions on scale in each photograph are  $0.01''$  apart.



Figure 10. High Quality BeO Crystals. (Run 920)

The crystal on the left grew on a  $[10.1]$  seed plate and is of the high quality, while that on the right grew on a  $[00.1]$  seed plate and is not as good in quality. (The smallest divisions are 0.01 inches.)



Figure 11. Ladder Assembly With Grown BeO Crystals  
at the End of Run (938).

The crystallographic orientations of the seeds used are: (1) cut  $[10.1]$  plate, (2) cut  $[11.1]$  plate, (3) platy crystal,  $(00.1)$ , (4) stubby crystal with pyramidal termination, (5) prismatic crystal with pyramidal termination, (6) cut  $[11.0]$  plate.

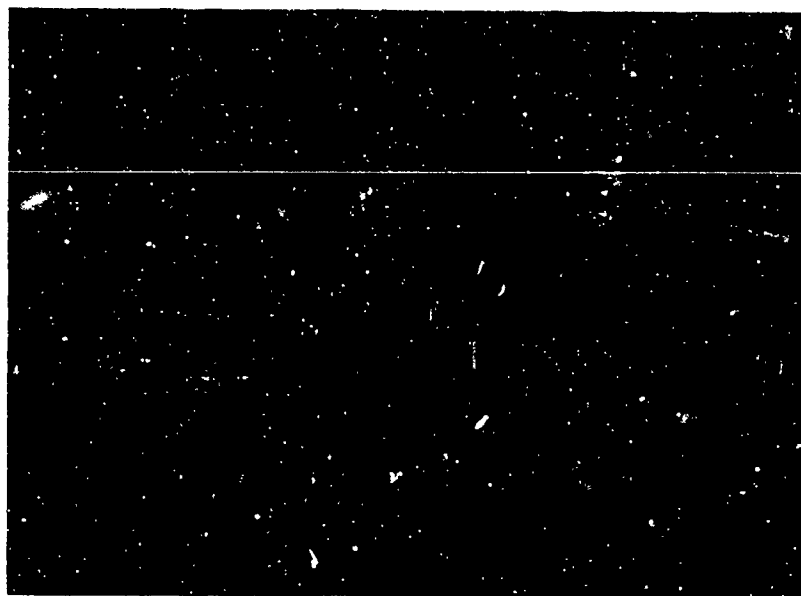


Figure 12. BeO Crystals Grown on  $[00.1]$  Seed Plates (Run 829).  
Crystal number 1 was used for slicing into  $[10.1]$  seed plates.



The feasibility of the meniscus between the liquid and vapor phases acting as a satisfactory baffle between the nutrient and growth zones was tested. In one run of thirty days duration, with the temperature in the nutrient zone at 586°C and the gradient to the growth zone 12°C, no mechanical baffle was installed. It was found that the seeds did not grow, and in fact, some dissolved, although small BeO crystals grew on the upper part of the walls. Growth on the seeds occurred in a previous run under similar conditions but with a mechanical baffle installed. This showed that two distinct isothermal zones were not formed simply by the presence of a meniscus. There was also the possibility that the convection pattern inside the vessel may be drastically affected by the design of a baffle used and the percent opening. These observations showed that some type of baffle is necessary in order to obtain satisfactory growth.

#### Effects of Impurities on the Crystals

It was observed that the extent of inclusion of silver in the crystals grown was related to the proximity of the crystals to the silver liner, and that the growth of silver dendrites occurred at the interface of the liquid and vapor phases. This indicated that silver was less soluble in the vapor than in the liquid phase. Our initial approach to solving the problem of the contamination of the crystals by silver has, therefore, been firstly to place the seeds in the central part of the vessel, and secondly to grow the crystals in the vapor phase rather than in the liquid. This has resulted in the lowering of the silver content of the crystals from 1000 ppm (Run 810) to <0.5 ppm (Run 880). The limit of detection of the spectrographic method used is 0.5 ppm. During the latter part of the investigation, it was learned that a group at Airtron had encountered a similar problem in their work on the hydrothermal growth of ZnO single crystals<sup>(9)</sup>. These workers attributed the cause of the corrosion of the silver to the presence of dissolved oxygen in the KOH solution, and solved this by suspending a piece of zinc metal in the KOH solution to scavenge the oxygen in the system. We have adapted this technique to our problem by suspending a strip of beryllium metal in the liquid in the lower part of the vessel to remove any free oxygen present in the system. To date none of these runs have been opened.

It was further observed that the amount of liquid which remained in the vessel at any particular temperature had a bearing on the quality of the crystal grown, and probably on the presence of some silver inclusions in the crystals. It is believed that this is due to the fact that when the level of the liquid present in the vessel during the run is low\*, the growth along the c-direction is more rapid relative to that in the direction perpendicular to it. When more liquid is present the growth perpendicular to the c-axis increases in speed and is of higher quality. Small

---

\*This was estimated from the position of the silver dendrites in the vessel, and the degree of fill of the autoclave. (see Figure 8).

silver dendrites are sometimes trapped in the inclusion in the poor quality crystals. It may be that the rate of diffusion of nutrient on the growing face may be the controlling factor here. The optimum condition for preventing these inclusions from occurring appears to be when the surface of the remaining liquid is somewhat below the level of the lowest crystal in the growth zone.

A run at 586°C developed a leak due to the solution of silver in the lower part of the liner by the KOH solution, with the formation of silver dendrites at the interface of the liquid and vapor phases. It was observed that the BeO crystals which formed in the liquid incorporated cobalt dissolved from the walls of the vessel. On the other hand, the crystals which grew in the vapor phase were free of the cobalt coloration. The cobalt contaminated BeO crystals had poorly developed faces which tended to be rounded. Attempts to modify the relative growth rates of the crystal faces by incorporating  $\text{PO}_4^{=}$  ions in the solution did not produce detectable results.

## Characterization of Crystals

Most of the work done in this direction was analytical and optical, because the more refined and sophisticated techniques are only valuable after the first order effects of chemical purity and obviously poor quality crystals have been solved. We are now beyond this stage and so our efforts will be more concentrated on the crystal perfection as can be measured by x-ray and other techniques.

X-ray Topography: The Berg-Barrett and/or the parallel beam method<sup>(10)</sup> reveals the density of dislocation and some angular misalignment in crystals. The lattice parameters when measured with high precision (approximately 1/100,000) will test the constancy of the unit cell dimensions from crystal to crystal. Detailed study of the line profile can be used to estimate micro-strain and mosaicity.

Lattice Parameters: The unit cell dimension a was calculated for each of the observed angles of the (300), and (200) peaks and the final value of a was arrived at by extrapolating the two observed values against  $\cos^2\theta/\sin\theta$ .

The measured a values for all of the crystals are precise since the (300) peak is at a high angle ( $\sim 163^\circ$ ,  $2\theta$ ), and further the expression for the a lattice parameter of a hexagonal crystal reduces to the following simple form using the (h0.0) peak

$$a = \frac{\lambda}{2h\theta} \cdot \frac{2}{\sqrt{3}} h$$

A major difficulty in determining the c value of BeO crystals is that the only natural faces which involve the c-dimension are 11.1 and 10.1. Both the (00.1) and (00. $\bar{1}$ ) faces were ignored here because they are usually small or absent. Since the (11.1) plane gives no reflections, only the (10.1) plane could be used. However, the values obtained showed wide variations and so were not acceptable. The problem was resolved by using polished (00.1) slices cut from the crystals grown. These gave the values listed below.

	$a_0$	$c_0$
Crystal 1	$2.6976 \pm 0.0002A$	$4.3780 \pm 0.0002A$
Crystal 2	$2.6977 \pm 0.0002A$	$4.3774 \pm 0.0002A$

In an attempt to improve the measurement the  $c$ -value was obtained from the (00.4), and (00.6) peaks of crystal 1.  $\text{CuK}_\alpha$  radiation was used. A tip of the crystal was placed in the beam, but it is not known with any certainty whether the reflection was from a face or a plane. The value obtained suggests that it was not. The value is,  $c = 4.3700\text{\AA}$ , (00.4) and (00.6).

The internal strains in the crystals were estimated by the degree of resolution of the  $K\alpha_1$ , and  $K\alpha_2$  doublet of the (20.2) peak ( $2\theta \sim 96^\circ$ ) and by comparing this with the (400) peak of a LiF single crystal ( $2\theta \sim 100^\circ$ ). The linear absorption coefficient of BeO is smaller than for LiF ( $\mu = 26$  for BeO;  $\mu = 34$  for LiF) so that the  $\alpha_2$  separation would not be expected to be as great in BeO as in LiF.

Elemental Purity: The results of the elemental analyses of BeO crystals grown on this project is given in Table 5. Spectrographic analyses of other BeO crystals reported in the literature are also given for comparison.

TABLE 5

SEMI-QUANTITATIVE SPECTROCHEMICAL ANALYSES OF BeO CRYSTALS

Element	Run 880 (1)	Hydrothermal (2)	Hydrolysis of $\text{BeF}_2$ (3)	$\text{PbF}_2\text{PbO}$ Flux <sup>2</sup> (4)
Ca	10 ppm	- ppm	20 ppm	- ppm
Al	< 20	-	60	-
Si	100	100	30	20
Ag	n.d.	-	-	-
Mg	10	-	30	-
Ti	n.d.	-	40	-
Na	n.d.	-	-	-
Fe	< 10	10	100	50
Pb	n.d.	-	-	100
F	-	-	1000	-
B	n.d.	7	-	10

1. BeO crystal from T.P.R. Run 880. Sought but not detected:  
Ni, Ag, Co, V, Ti, Sr, Zr, Cu, Ba, Mn, Sb, Sn, Ge, Ca.  
(Norman Shur, Analyst)
  2. Newkirk and Smith <sup>4</sup>
  3. Newkirk and Smith <sup>4</sup>
  4. Newkirk and Smith <sup>4</sup>
- n.d. = not detected

The BeO crystals obtained in Run 92C (Figure 10) were examined without any preliminary preparation, i.e., they were neither polished nor etched. The Berg-Barrett apparatus used was similar to that described by Austerman<sup>(10)</sup>. The diffraction image was recorded on Kodak Spectroscopic Film. Photographs

were taken of the (10.1) face of the first crystal (platelet) and of the (100), faces of the second crystal (hexagonal outline). Photographs of the crystals were taken through a microscope while Berg-Barrett enlargements were obtained by direct enlargement of the spectroscopic film. Figures 13-17 illustrate the results.

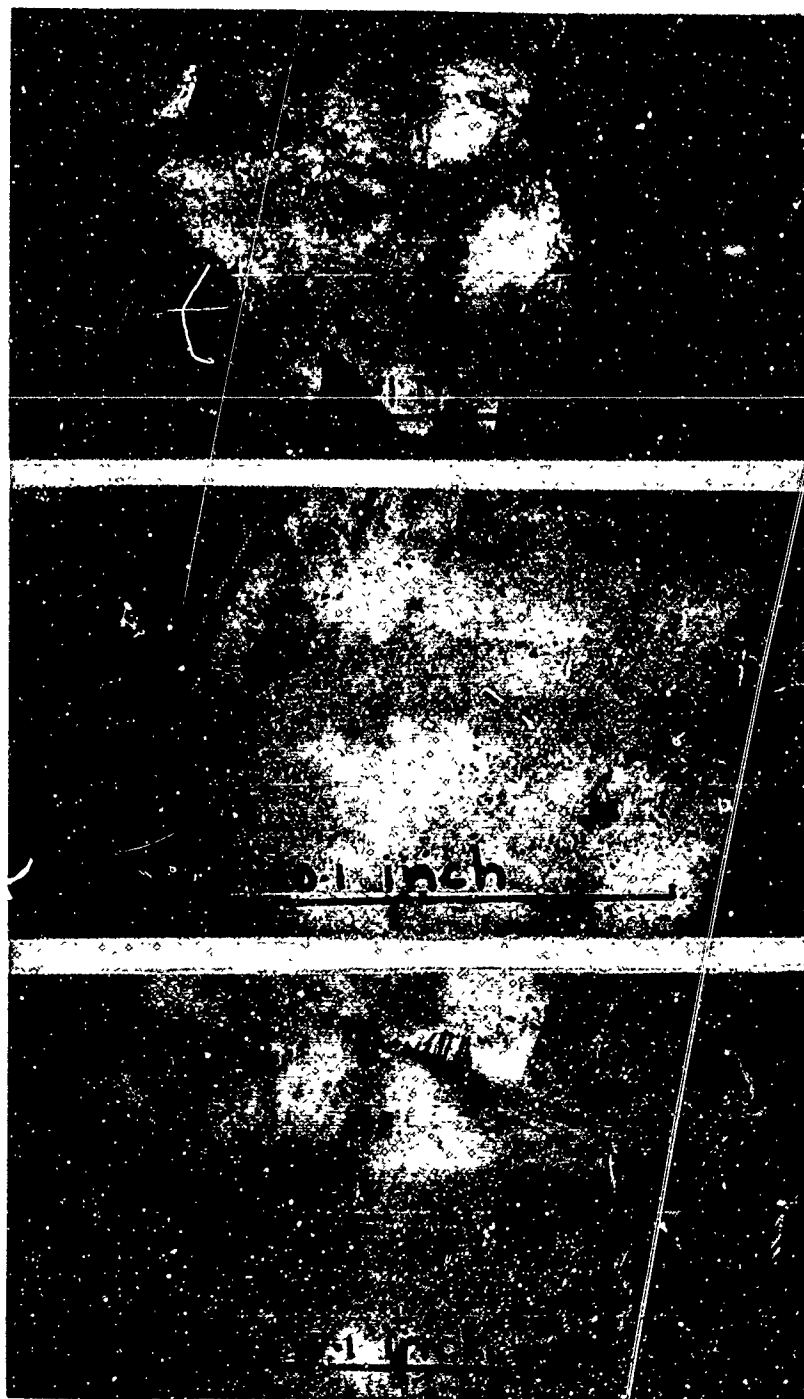


Figure 13. Optical Photographs of (101) Face of Crystal 1,  
Figure 10 (see page 10).

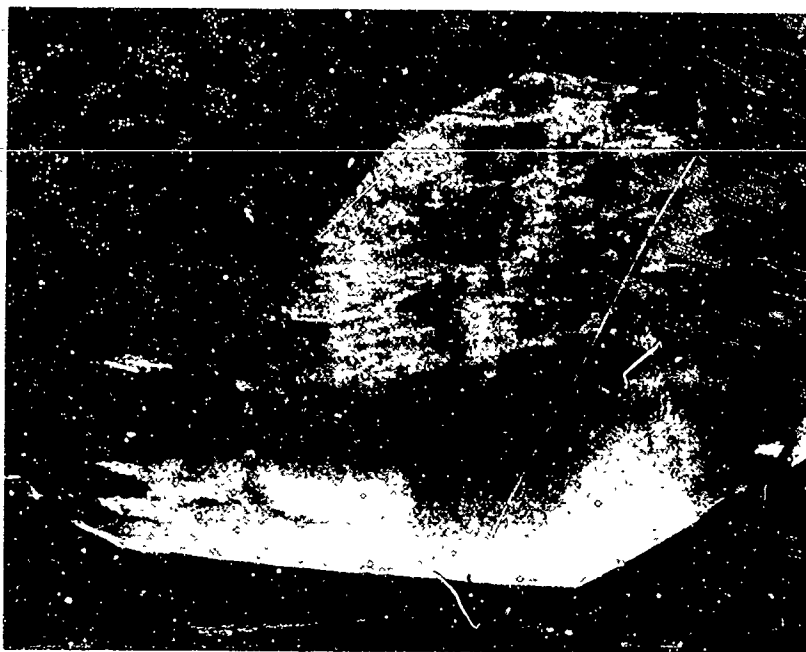


Figure 14. Berg-Barrett Photograph of (10.1) Face of Crystal 1, Figure 10 (see Figure 13).

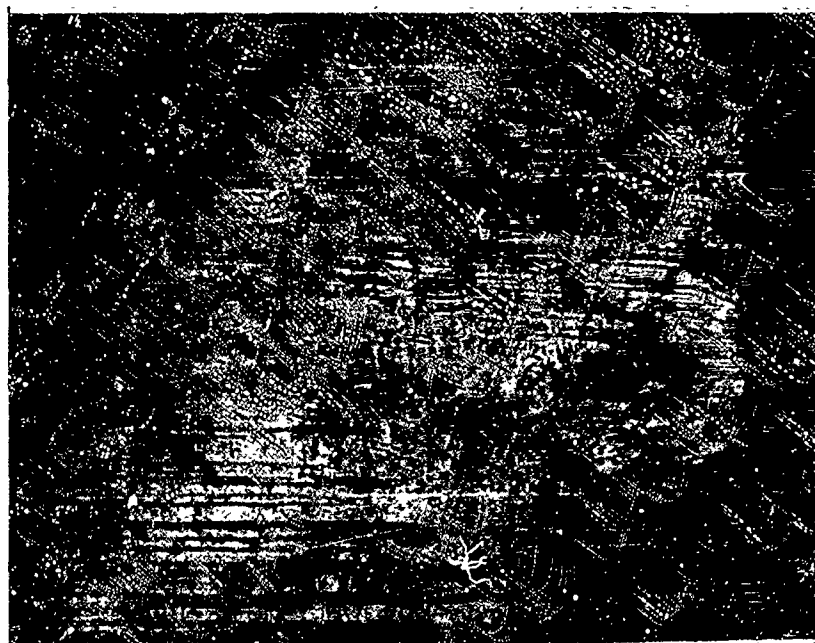
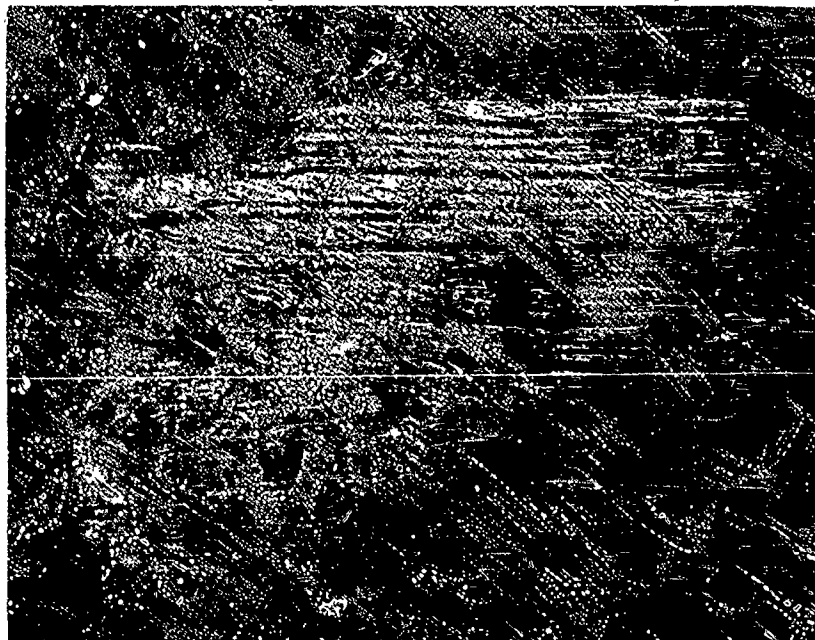


Figure 15. Optical Photograph of (10.0) Face of Crystal 2,  
Figure 10.



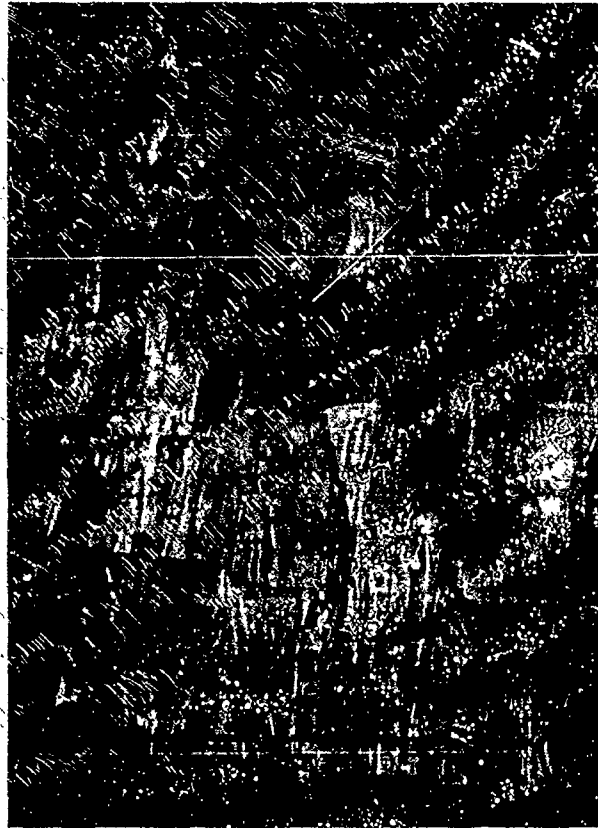


Figure 16. Optical Photograph of Adjacent (10.0) Face  
of Crystal 2, Figure 10.

The black hexagonal figure is a small negative inclusion at the surface of  
the crystal.

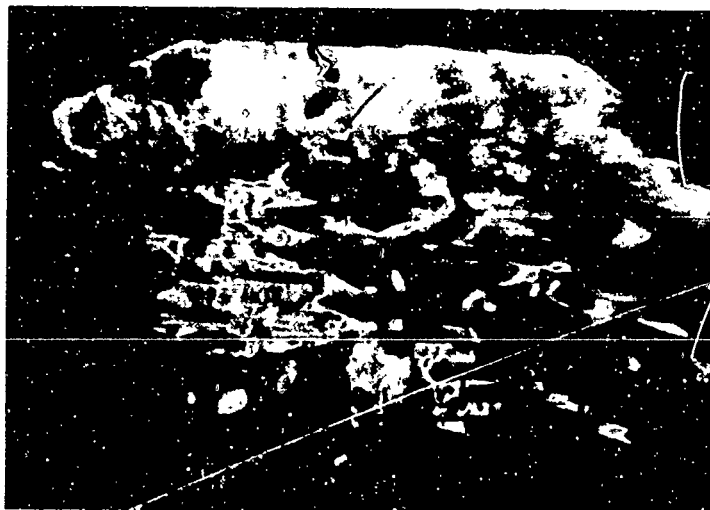


Figure 17. Berg-Barrett Photograph of (10.0) Face  
of Crystal 2 Figure 10.



Figure 18. Berg-Barrett Photograph of Part of  
Figure 17 Enlarged.

## VI. DISCUSSION OF RESULTS

Perhaps the most significant observation made in relation to the hydrothermal growth of BeO crystals is that it is the positive pyramidal termination which is nucleated. This means that the orientation of the seed must be such that the nucleation on this plane will not cause the crown type growth which occurs when the (00.1) orientation is exposed for growth. To minimize this, the rate of growth of the seed must be such that few of these are nucleated and these spread out rather than form spires. The use of the [11.0] and [11.1] seed plates would seem to encourage this type of growth. The former is not a naturally occurring face, while the latter occurs very rarely, so both of these would be expected to be relatively good planes for this purpose. These seed plates along with others were used in Run 938 (Figure 11). This run confirmed that the relative growth rates in the various directions are:

$$[11.0] > [00.1] \approx [00.\bar{1}] > [11.1] > [10.1] > [10.0].$$

Because of the varying quality of the seeds used, we cannot at this time unequivocally determine the effects of the seed orientation of the quality of the crystals produced, but tentatively these seem to be:

$$[10.1] \approx [11.1] > [11.0] \approx [10.0] > [00.1] \approx [00.\bar{1}].$$

Perhaps the most important factor affecting the quality of the crystals grown is the quality of the seeds used. This has been well demonstrated in runs 920 (Figure 10) and 938 (Figure 11), and is summarized qualitatively in Table 6.

TABLE 6  
EFFECTS OF SEED QUALITY ON OVERGROWTH

Run No.	Orientation	Seed Quality	Crystal Quality
920	(00.1)	fair	good
	(10.1)	v. good	v. good
938	(10.1)	poor	fair
	(11.0)	poor	fair
	(11.1)	poor	fair

Another possibility of improving the quality of the crystals was tried with the (11.0) and (11.1) seed plates. This is the use of  $\text{PO}_4^{\equiv}$  ions which are reported to encourage lateral growth<sup>(4)</sup> (Run 932). We have observed that under hydrothermal conditions the addition of these ions to the solution did not have the reported effects. Perhaps the reason for the lack of effectiveness of these additives may be that they may be preferentially partitioned in the liquid phase rather than in the vapor phase where the crystal is growing. On the other hand, the hydrothermal solution

had similar effects as those reported for the addition of boron oxide to a melt. That is, it reverses growth polarity, and increases growth rates in the positive polar direction.

One advantage of the hydrothermal method is the fact that the growing crystal is able to reject impurities present in the nutrient. Table 1 shows that the BeO pellets used as nutrient were contaminated with Ca, Mg, Al, and Si during the fabrication process. It is, however, significant that of these only Si was incorporated in the growing crystal to any extent and even here it was significantly reduced as compared to the level present in the nutrient. This is important because we have demonstrated that in the production growth of BeO it may not be necessary to use ultra-pure BeO and so a reduction in cost may be achieved by this.

The high quality of the crystals grown in Run 920 (Figure 10) is demonstrated by the x-ray topographic studies done so far. The surface of the first crystal is not as rough as that of the second crystal as is evidenced by the optical photograph (Figures 13 and 15). The left hand side of the Berg-Barrett photograph (Figure 14) has details which could not be due to dislocations since examination of the optical picture reveals no surface defects which might cause this. Consider the (10.1) face of crystal 2 (Figures 16-17). The Berg-Barrett analysis shows that the crystal has not diffracted as a whole but rather in patches. Figure 18, which is a photographic enlargement of a part of Figure 17 clearly demonstrates this lack of uniform diffraction by the crystal as a whole. Upon examination of the optical pictures of the crystal, the rough surface is readily evident. There are steps all along the surface of the crystal. This would in part explain the patchy diffraction patterns as the result of the steps, which would break up the surface of the crystal into various areas, thereby preventing diffraction as a whole. The condition of the surface, then prevents an unambiguous study of the defect state of the crystal.

One of the unique features of this work is the fact that the crystals are grown in a dense vapor phase above the liquid phase containing the nutrient. A baffle is, however, necessary to separate the vessel into two isothermal zones. The lower nutrient zone contains a liquid phase and a vapor phase above it. The upper growth zone contains entirely a vapor phase. The recrystallization process substantially improves the purity and quality of the crystals grown.

The estimation of the internal strain in the crystal by the degree of resolution of the  $K\alpha_1$  and  $K\alpha_2$  doublet showed that there was a small but noticeable difference between BeO and the LiF reference crystal. This demonstrated that the strain present in the BeO crystal was qualitatively small.

## VII. CONCLUSIONS

The work done so far has conclusively demonstrated that high quality BeO crystals can be grown hydrothermally. The major obstacle to the routine production of these crystals is that of obtaining high quality seeds. Crystals weighing up to 1.07 g. have been grown hydrothermally in four molar potassium hydroxide solution with the nutrient temperature of  $535 \pm 5^\circ\text{C}$ , and growth zone temperature of  $505 \pm 5^\circ\text{C}$ . The best quality crystals were also obtained under similar conditions, but in this case high quality seeds were used.

The purest crystals were grown in a dense vapor phase above the liquid which contained the nutrient material. This is the first time that a large crystal has been grown hydrothermally from a vapor.

#### VIII. FUTURE WORK

The characterization of the hydrothermally grown BeO crystals is the major area where much more work remains to be done. However, additional large crystals are necessary to do this satisfactorily. Work on growing these crystals has already been started, but it will be necessary to slice some of these crystals to provide larger seeds for use in other long term growth runs. The characterization of the crystals grown will then be done using the techniques described. These will be supplemented with the study of their absorption spectra. This is a particularly valuable tool for detecting the presence of (OH-) and also differentiating it from free water.

Further work is also underway on the characterization of the BeO crystals for defects and structural perfection. This involves the polishing of the parts of various faces to remove the effect of surface features which make the interpretation of the Berg-Barrett photographs somewhat difficult.

## IX. REFERENCES

1. A. A. Ballman, and R. A. Laudise; Hydrothermal Growth; The Art and Science of Growing Crystals; John Wiley and Sons, Inc., New York, (1963), pp. 231-251.
2. S. B. Austerman; Growth of Beryllia Single Crystals; J. Am. Ceram. Soc., Vol. 46, (1963), pp. 6-10.
3. H. W. Newkirk, and D. K. Smith; Studies of the Formation of Crystalline Synthetic Bromellite. I. Microcrystals; Am. Min., Vol. 50, (1965), pp. 22-43.
4. H. W. Newkirk, and D. K. Smith; Studies of the Formation of Crystalline Synthetic Bromellite. II. Macrocrystals; Am. Min. Vol. 50, (1965), pp. 44-72.
5. H. W. Newkirk; The System BeO-H<sub>2</sub>O at Moderate Temperatures and Pressures; J. Inorg. Chem., Vol. 3, (1964), pp. 1041-1043.
6. V. G. Hill and R. I. Harker; Development of Hydrothermal Method for Growing Single Crystals of High Purity Beryllium Oxide, and Lead Metaniobate; Tech. Rep. No. AF ML-TR-65-297, (1965).
7. W. W. Webb; X-ray Diffraction Topography; Direct Observations of Imperfections in Crystals; J. B. Newkirk and J. W. Wernick, editors, Interscience, (1962), pp. 29-76.
8. H. E. Swansen and E. Tatge; Standard X-ray Diffraction Powder Patterns; N. B. S. Circular 529, (1953), p. 26.
9. Rock R. Monchamp and Richard C. Puttback; The Hydrothermal Growth of Zinc Oxide Crystals; Tech. Rep. No. IR-7-988(11).
10. S. B. Austerman, J. B. Newkirk and D. K. Smith; Study of Defect Structures in BeO Single Crystals by X-ray Diffraction Topography; J. Appl. Phys., Vol. 36, (1965), pp. 3815-3822.

## CHAPTER 2. POTASSIUM TANTALATE-NIOBATE (KTN) $\text{KTa}_{0.65}\text{Nb}_{0.35}\text{O}_3$

### I. INTRODUCTION

The present revived interest in potassium tantalate-niobate is mainly due to the observation of Geusic et al<sup>(1)</sup> that this material has very useful electro-optical properties when the device is operated just above the Curie temperature ( $T_C$ ), and the material is in the cubic paraelectric state. Under these conditions it has the added advantages that the electro-optical effect is quadratic, and when the crystal is biased with readily obtainable voltages it can be driven by transistor circuitry to perform the optical modulation function. Besides these advantages, KTN has excellent acoustical parametric amplification characteristics.

The fact that the material has these desirable properties led to the intense study and development of that composition in the solid solution series, which has the  $T_C$  at or just below room temperatures. This permits a device capable of producing large polarizations to operate at room temperatures. The composition  $\text{KTa}_{0.65}\text{Nb}_{0.35}\text{O}_3$  (KTN) was, therefore, selected as the most desirable, (Figure 19).



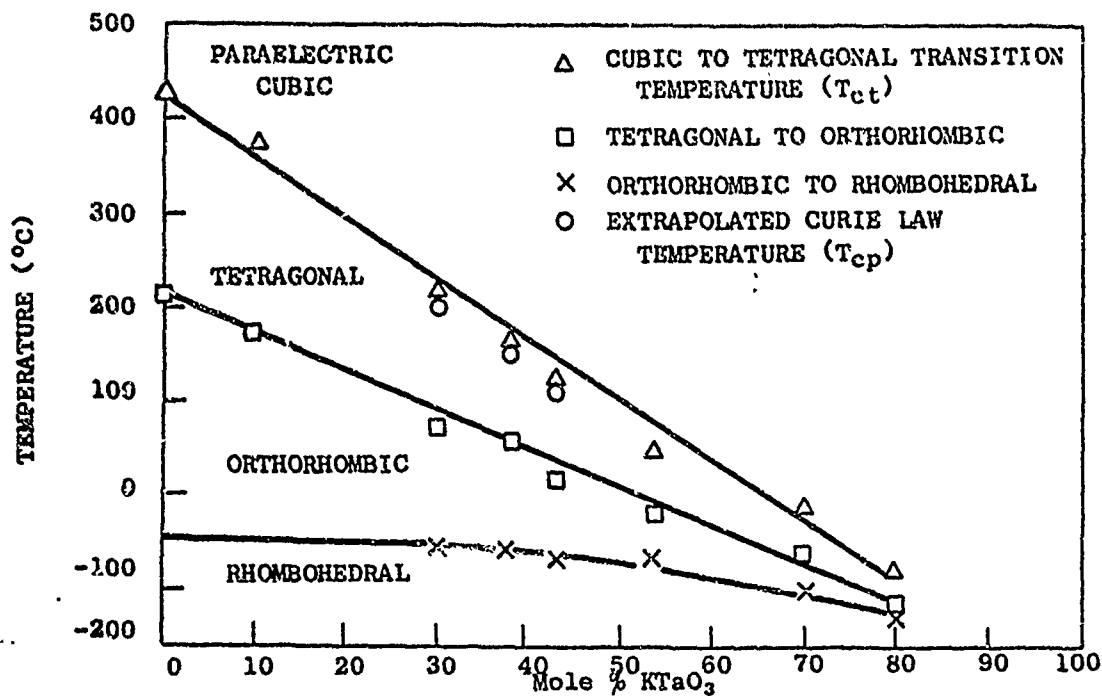


Figure 19. Transition Temperatures and  $T_{cp}$  as a Function of Composition in  $\text{KTaO}_3$ - $\text{KNbO}_3$  Solid Solution (5).

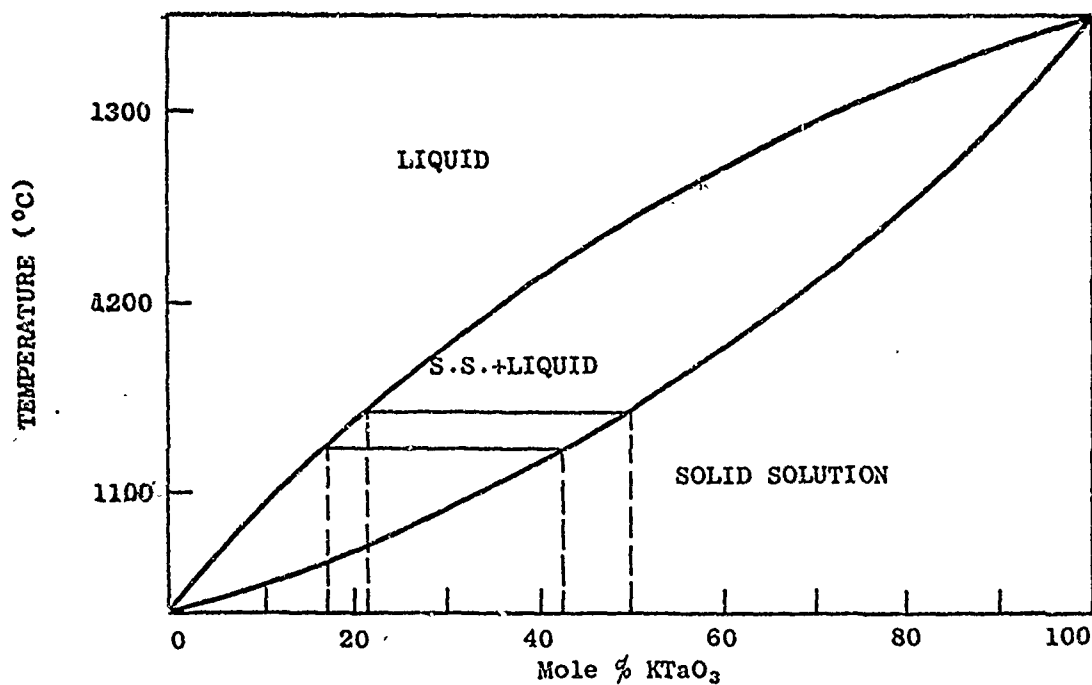


Figure 20. Phase Diagram for the System  $\text{KNbO}_3$ - $\text{KTaO}_3$ . (6)

## II. PREVIOUS WORK

Attempts to grow crystals of this composition have been made by Bonner et al<sup>(2)</sup>, and Wilcox and Fulmer<sup>(3)</sup> using flux methods; and Marshall and Laudise<sup>(4)</sup> using hydrothermal methods. However, the crystals produced so far have not been entirely satisfactory because they develop a lamellar pattern, which is believed to either represent areas of slightly different Nb/Ta ratios, and hence different structures at room temperatures, or domain structures. There is also the additional difficulty of preventing zoning in the crystals, as is indicated by the wide loop between the solidus and liquidus curves of the system  $\text{KNbO}_3\text{-KTaO}_3$  (Figure 20). This difficulty can be minimized by using a large charge, stirring the melt efficiently and crystallizing out only a relatively small amount of material. It is, however, desirable to develop a method of growing these crystals that would be free of these lamellar patterns, which are the reasons for the rejection of a very high percentage of the crystals grown.

The growth of the crystals in the subsolidus region of the system would seem to offer a possible alternative for obtaining crystals of the desired composition, and free of the lamellar pattern and other defects. The hydrothermal method, which essentially operates under these conditions, therefore, warrants investigation. Marshall and Laudise<sup>(4)</sup> in their study of the solid solution series  $\text{K(Ta,Nb)O}_3$ , found that there was a dependence of the unit cell size, and hence composition and Curie temperature, upon crystallization temperature and KOH concentration. This suggests the need for precise control of the growth temperature to produce crystals of uniform and stoichiometric composition.

### III. APPROACH

The first objective was to determine the equilibrium phase relationships in the system below the solidus. Reisman, Triebwasser and Holtzberg<sup>(6)</sup>, Garn and Flaschen<sup>(7)</sup> and Wilcox and Fulmer<sup>(8)</sup> reported that a complete solid solution series existed in the system  $\text{KNbO}_3$ - $\text{KTaO}_3$  at liquidus temperatures, but no information was found on the equilibrium relations in the subsolidus region. This information is vital for the hydrothermal growth of KTN crystals, since this method tends to promote more rapid attainment of equilibrium conditions.

It was also necessary to obtain at least a rough estimate of the effects of the hydrothermal environment on the liquidus temperatures in the system, since it was expected that the hydrothermal solution would lower the liquidus temperatures, and so impose a maximum temperature under which the crystals could be grown hydrothermally. The initial work had established that  $\text{KNbO}_3$ - $\text{KTaO}_3$  solid solution has only a limited solubility in water or KOH solutions at lower temperatures. This lower solubility has some advantages since if only a small amount of the solid phase is dissolved in the solution, then a large reserve of nutrient material will be available to keep the composition of the liquid phase constant. There is, therefore, the possibility of maintaining a constant composition in the crystals which precipitate from the solution, and so avoid the problems found when the crystals are grown from a flux.

#### IV. EXPERIMENTAL

##### Starting Materials

The chemicals used were  $Ta_2O_5$ ,  $Nb_2O_5$ , and KOH (manufacturers stated purity 99.9%). Stoichiometric mixtures of  $KTaO_3$ ,  $KNbO_3$ , and compositions between these including  $KTa_{0.65}Nb_{0.35}O_3$  were prepared by weighing together the required amounts of  $K_2CO_3$  and the oxides, which had been previously dried at 400°C. These were homogenized by grinding in an agate mortar using acetone as the suspending agent. The mixtures were air dried until free of acetone and then stored. Portions of these mixtures were also heated to 600°C for 48 to 72 hours and then to 800°C for one hour to produce a very fine grained KTN which is very reactive and suitable for use in phase equilibrium studies. Another portion of the mixture was fired to 1300°C in a sealed Bridgman crucible, and crystallized. This produced a coarsely crystalline material which was used in some runs.

##### Equipment and Techniques

The hydrothermal equipment used in these experiments included the standard Tem-Pres hydrothermal research units Model HR-1B, which have been described in previous reports(8). The autoclaves were the test tube type of 1/4 and 1/2 inch inside diameter, and were fabricated of René or Stellite alloys. In both cases, the charge and the required amount of the solution selected were sealed inside gold capsules. These were placed in the autoclaves, and brought to the operating conditions of temperature and pressure. The furnaces were removed from the autoclaves at the end of the run and the autoclaves were water quenched. Dry runs were made by firing previously decarbonated mixtures either in sealed platinum tubes, or in covered platinum buckets at temperatures between 400°C and 1000°C for from two to five days.

The petrographic microscope proved to be a valuable tool for the identification of the phases obtained. This, however, had to be supplemented by x-ray diffraction studies, because of the presence of different polymorphs, and the very fine particle size of many of the crystals. A Tem-Pres Model XD-1 x-ray diffractometer was used. The shift in certain high angle peaks was used for the determination of solid solution. Similarly the appearance of lines of a second phase (Nb or Ta rich) or the presence of another polymorph was used as the basis for deciding on the limits of solid solution in the sub-solidus part of the system.

An Applied Research Laboratory electron probe was also used to study composition variation across the faces and in slices of the crystals grown.

##### Subsolidus Phase Relations in the System $KNbO_3$ - $KTaO_3$

The subsolidus phase relations in the system  $KNbO_3$ - $KTaO_3$  are shown in Figure 21 based on experimental data indicated. On the Ta-rich side, the solid solubility increases from 22.3 mole% at 700°C to a little less than 50 mole% at 1000°C, but the range of solid solution in the Nb-rich side is limited to less than 10 mole % over the entire temperature range, at pressures up to 1,000 bars.

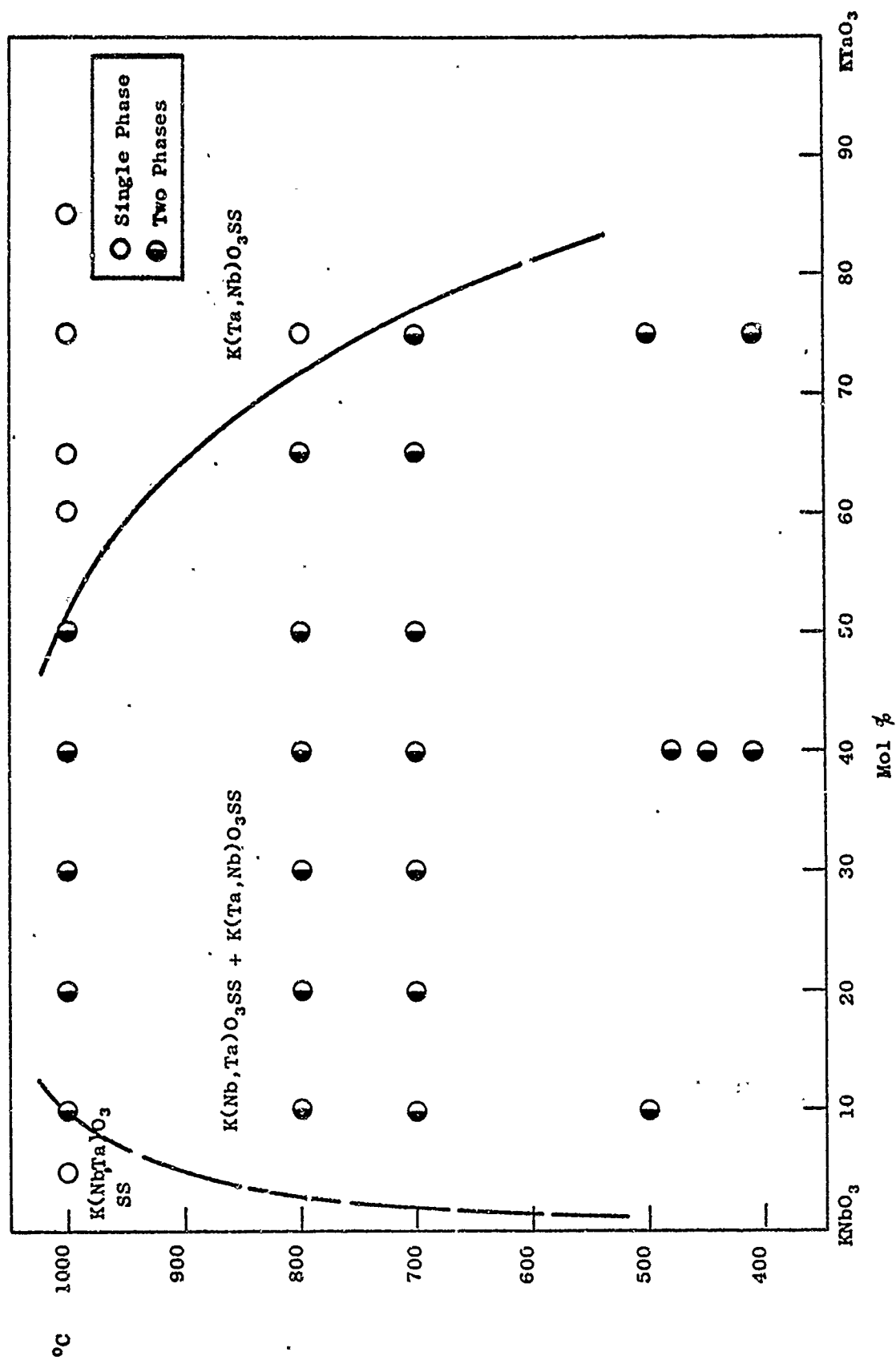


Figure 21. Subsolidus Equilibrium Phase Relations in the System  $\text{KNbO}_3$ - $\text{KTaO}_3$ .

The x-ray diffraction patterns from crystals of  $\text{KTaO}_3$  and  $\text{KNbO}_3$  are very similar, although  $\text{KNbO}_3$  shows splittings of several major peaks due to nonquenchable phase changes. However, an immiscibility gap can be detected if high-angle x-ray reflections are used. The similarity in cell dimensions of  $\text{KTaO}_3$  and  $\text{KNbO}_3$  makes the shifts of reflections as a function of composition in the low angle range so insignificant that a false impression of complete series of solid solution is usually given.

So far, self-nucleated crystals up to 3 mm on edge have been grown in runs made to study the location of the exsolution dome (Figure 22).

The color of the crystals grown varied from colorless to pale blue. It appeared that the crystals grown at higher temperatures were clearer than those at lower temperatures but other factors are undoubtedly involved. In a few cases, pale brown crystals were produced, and we concluded that the redox potential in the system affected the color of the crystals.

The smaller KTN crystals, and those formed at lower temperature, were usually free from lamellar patterns. However in some runs, particularly those made at higher temperatures exsolution patterns were observed in the crystals. These appeared as criss-cross patterns associated with cleavage and were usually about 0.005 mm across (Figure 23). When viewed under crossed nicols it was observed that the striation lines were anisotropic, suggesting that they were niobium rich areas (Figure 24).

In an attempt to verify the presence of the exsolution dome in the system, sections of flux grown KTN\* crystals were treated hydrothermally in 8N-KOH solution at 765, 665 and 583°C and 1,000 bars. The first was for four days, and the others for 10 days. The section which was treated at 765°C has the edges and a part of the two other faces partially coated with tiny crystals in optical continuity with the rest of the crystal. The section treated at 665°C showed minor recrystallization while the third showed no change.

No systematic study of the solubility of KTN in various solvents was made because the phase relationships showed the presence of the exsolution dome.

#### Compositional Variations in Crystals

Because the petrographic microscope showed cleavage zones, with what appeared to be exsolution areas rather than domain structures, an attempt was made to confirm if these areas were niobium rich with respect to the rest of the crystal. Two spectrometers on the Applied Research Laboratory electron probe unit set at wave lengths of Ta  $L\alpha$  1.5256Å and Nb  $L\alpha$  , 5.724Å

---

\*The crystals were kindly supplied by Speedway Laboratories, Linde Division, Union Carbide Corporation.

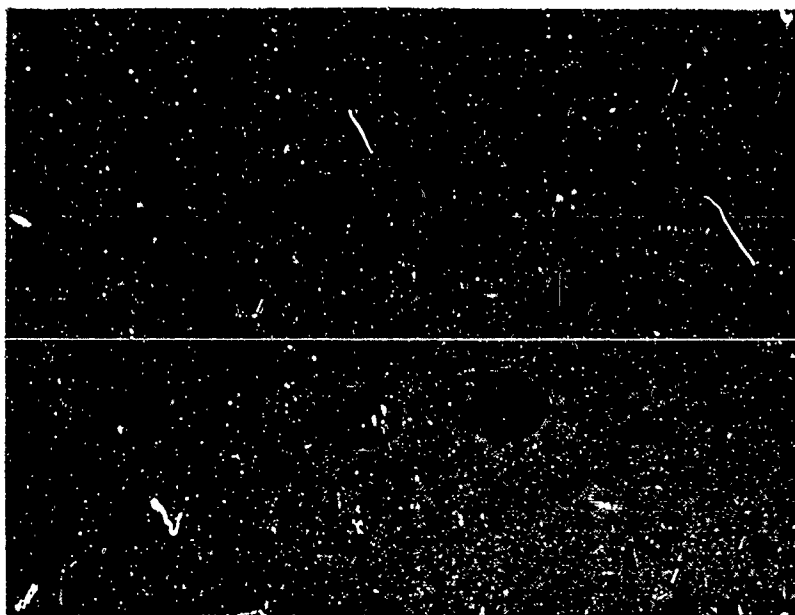


Figure 22. Largest KTN ( $\text{KTa}_{.75}\text{Nb}_{.25}\text{O}_3$ ) Crystals Grown Hydrothermally  
(Run 93<sub>2</sub>)

\*The smallest scale divisions are 0.01 inches.



Figure 23. Exsolution Pattern in KTN Crystals Grown in Run 924 - Polarized Light

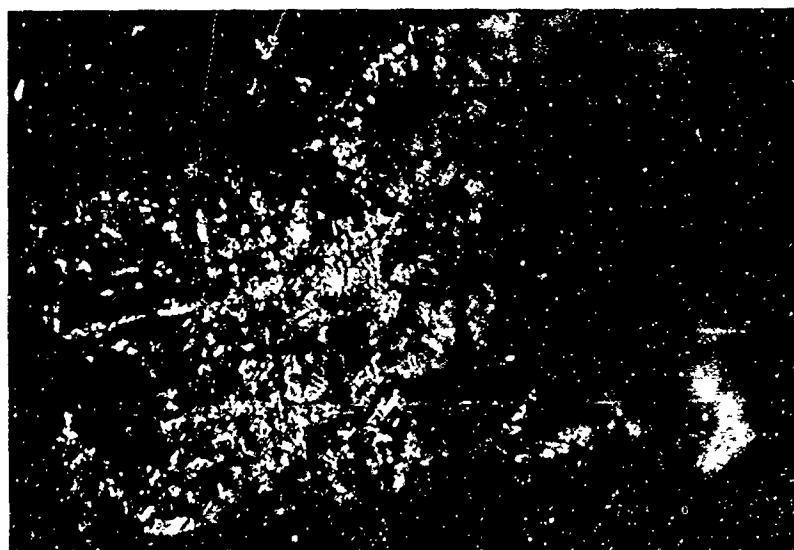


Figure 24. Exsolution Pattern in KTN Crystals Grown in Run 924 - Crossed Nicols.



were used. The acceleration voltage was 30 K e.v. with a sample current of 0.03 amp . The spot size was 1-2  $\mu$  diameter, and the scanning speed 96  $\mu$ /minute. An electron probe traverse across a (100) cleavage face showed that the niobium content in the cleavage areas appear to be slightly richer than in the rest of the crystal, but this could not be verified with any certainty, because of the small size of these zones. However, when the crystal face was polished no differences were detected in the Nb/Ta ratio, except towards the edges. Here the tantalum content decreased substantially and the niobium content increased.

The Nb/Ta ratio across the lamellar pattern of the KTN crystals supplied by Speedway Laboratories were also studied under the same conditions. The ratio was found to be relatively uniform across most of the crystal, but one area near the edge of the crystal showed a Nb rich zone.

## V. DISCUSSION OF RESULTS

The presence of an exsolution dome in the system is the novel result of this study. Although this is not surprising, previous attempts to grow single crystals of this material had not taken this possibility into account. This is somewhat surprising because most of the difficulties encountered in obtaining high quality KTN single crystals are best accounted for by the presence of such a dome. It should be remarked that the exsolution rate in the system is sluggish, and so it may be possible to obtain single phase KTN crystals at room temperature by careful control of growth conditions. In fact, the electron probe study of many of the crystals obtained so far suggest that this is a distinct possibility. The hydrothermal growth of KTN crystals is, however, not feasible with the equipment currently available; since homogeneous  $\text{KTa}_{.65}\text{Nb}_{.35}\text{O}_3$  crystals can only be grown at temperatures above  $900^\circ\text{C} \pm 10^\circ\text{C}$ . The upper recommended limit of currently available large capacity autoclaves fabricated of René is  $700^\circ\text{C}$ .

## VI. CONCLUSIONS

This study has shown that the KTN composition  $\text{KTa}_{.65}\text{NbO}_{.35}\text{O}_3$  is metastable at temperatures below  $900 \pm 20^\circ\text{C}$ , and so it is not feasible to grow crystals of this composition hydrothermally. It is suggested that better crystals can be obtained from the melt by more careful control of the temperature to minimize the possibility of the crystal exsolving.

## VII. REFERENCES

1. Geusic, J. E., Kurtz, S. K., Van Uitert, L. G., and Wemple, S. H., Electro-optic Properties of Some  $ABO_3$  Perovskites in the Para-electric Phase, J. Appl. Phys. Letter 4, (1964), pp. 141-143.
2. Bonner, W. A., Dearborn, E. F., and Van Uitert, L. G., The Growth of KTN Single Crystals for Optical Applications, Bull. Am. Ceram. Soc., Vol 44, (1965), pp. 9-11.
3. Wilcox, W. R., and Fulmer, L. D., Some Factors Affecting the Growth Properties of  $KTaO_3$ - $KNbO_3$  Mixed Crystals, SSD-TR-65-68, J. Am. Ceram. Soc., Vol. 48, (1966), pp. 415-418.
4. Marshall, D. J. and Laudise, R. A., The Hydrothermal Phase Diagrams  $K_2O$ - $Kn_2O_5$  and  $K_2O$ - $Ta_2O_5$  and the Growth of Single Crystals of  $K(Ta,Nb)O_3$ , Abstracts I.C.C.G., Boston, (1966), pp. 66.
5. Treibwasser, S., Study of Ferroelectric Transitions of Solid Solution Single Crystals of  $KNbO_3$  and  $KTaO_3$ , Phys. Rev., Vol. 114, (1959), pp. 63-70.
6. Reisen, A., Treibwasser, S., and Holtzberg, F., Phase Diagram of the System  $KNbO_3$ - $KTaO_3$  by the Methods of Differential Thermal and Resistance Analysis, J. A. C. S., Vol. 77, (1955), pp. 4228-4236.
7. Garn, P. D., and Flaschen, S. S., Analytical Application of the D. T. A., Anal. Chem., Vol. 29, (1957), pp. 271-275.
8. Hill, V. G., and Harker, R. I., Development of Hydrothermal Method for Growing Single Crystals of High Purity Beryllium Oxide and Lead Metaniobate, AFML-TR-65-297, Tech. Rep. U. S. Air Force, (1965).

## CHAPTER 3. CHRYSOBERYL

### I. INTRODUCTION

Because of its similarity to both ruby and spinel, the chrysoberyl structure is an interesting host lattice into which various transition metal ions may be substituted and their optical, magnetic, and chemical properties measured. This is illustrated by the gem variety alexandrite, which has chromium substituting for aluminum. This mineral has a very characteristic absorption spectrum and is strongly dichroic, shining green in the day light and purple-violet under incandescent light. Large high quality crystals of this material are, therefore, desirable for the measurement of their physical properties.

From the crystal growing standpoint, chrysoberyl is also an interesting double oxide to grow, because the two components  $\text{BeO}$  and  $\text{Al}_2\text{O}_3$  are relatively similar chemically, and so problems due to their unequal partition between the solution and the crystalline phase should be minor in dilute to moderately strong alkaline solution. Besides this, the solubilities of both of these oxides have been determined in different solutions at elevated temperatures and pressures. A detailed determination of how the double oxide behaves should, therefore, add to our basic knowledge of hydrothermal crystal growing processes.

## II. PREVIOUS WORK

Chrysoberyl is a stable phase in the system  $\text{BeO-Al}_2\text{O}_3$ . This binary was first investigated by Wartenberg and Reusch<sup>(1)</sup>, who, however, did not find its stability field. Geller, et al<sup>(2)</sup>, re-investigated the system and located its stability field and determined the melting point to be  $1890^\circ\text{C}$ . Later Foster and Royal<sup>(3)</sup> studied the system  $\text{BeO-Al}_2\text{O}_3\text{-Al}_2\text{O}_3$  and found another phase with the probable formula  $\text{BeO}\cdot 3\text{Al}_2\text{O}_3$ . Lang, et al<sup>(4)</sup>, repeated this work and confirmed that  $\text{BeO}\cdot 3\text{Al}_2\text{O}_3$  was a stable phase in the system and that it has a melting point of  $1910 \pm 10^\circ\text{C}$ . Another new phase with the formula  $3\text{BeO}\cdot\text{Al}_2\text{O}_3$  was reported to exist in the system by Galakhov<sup>(5)</sup>. This latter compound is very similar optically to chrysoberyl, but it is readily distinguishable from it by its x-ray diffraction pattern.

The synthesis of chrysoberyl has been described by Palache, et al<sup>(6)</sup>, but attempts by Farrell and Fang<sup>(7)</sup> to duplicate this were unsuccessful. These latter authors, however, reported on the flux growth of both chrysoberyl ( $\text{Al}_2\text{BeO}_4$ ) and alexandrite ( $\text{Al}_2\text{BeO}_4\text{:Cr}$ ). They obtained chrysoberyl crystals between 0.1 and 10.0 mm from flux of the composition  $\text{PbO}$  66.6,  $\text{Al}_2\text{O}_3$  16.7, and  $\text{BeO}$  16.7 mole per cent.

### III. EXPERIMENTAL

#### Equipment

The equipment used for the solubility determinations and preliminary crystal growing runs consists of two Tem-Pres hydrothermal research units, Model HR-1B. These have been described fully in the Technical Report No. AFML-TR-65-29<sup>(8)</sup>.

#### Starting Materials

The BeO used in making the mixtures was purchased from Gallard-Schlesinger Chemical Mfg. Corp., Carle Place, L. I., N. Y., to be 99.9% pure, while the  $\text{Al}_2\text{O}_3$  used was obtained from Fisker Certified Aluminum Hydroxide ( $\text{Al}_2\text{O}_3 \cdot n\text{H}_2\text{O}$ ). This was ignited at  $1100^\circ\text{C}$  to determine the alumina content of the material. Equimolar mixtures of  $\text{Al}_2\text{O}_3$  and BeO were prepared, thoroughly mixed by grinding, ignited slowly to  $500^\circ\text{C}$  and then half an hour at  $1300^\circ\text{C}$ . When cooled, the powder was formed into pellets by mixing with 10% Carbowax solution in water to a crumbly consistency. About 12-15 mg of the powder was placed in a 0.125 inch diameter pellet press and compressed to about 30,000 p.s.i. The green pellets were dried at  $100^\circ\text{C}$ , cleaned by scraping from the surface any dirty marks due to press contamination, fired overnight at  $400-500^\circ\text{C}$  and finally at  $1300^\circ\text{C}$  for half an hour. This method produced strong well-sintered pellets.

#### Procedures

Solubility determinations of  $\text{Al}_2\text{BeO}_4$  were made in water and 1 to 8 normal KOH and NaOH solutions at temperatures between  $100$  and  $800^\circ\text{C}$  and pressures up to 4,000 bars. The techniques used were similar to those previously described<sup>(1)</sup>.

#### Results

The results of the solubility determinations of chrysoberyl in KOH solutions at 1,000 bars and those in water at 4,000 bars are given in Figure 25. Small crystals of chrysoberyl were obtained in a few runs with 6N-KOH as solvent, while runs with 8N-KOH gave another phase. There were, however, too few of these small crystals to permit identification. No crystals were obtained in runs containing 1 to 4N-KOH or water as solvent.

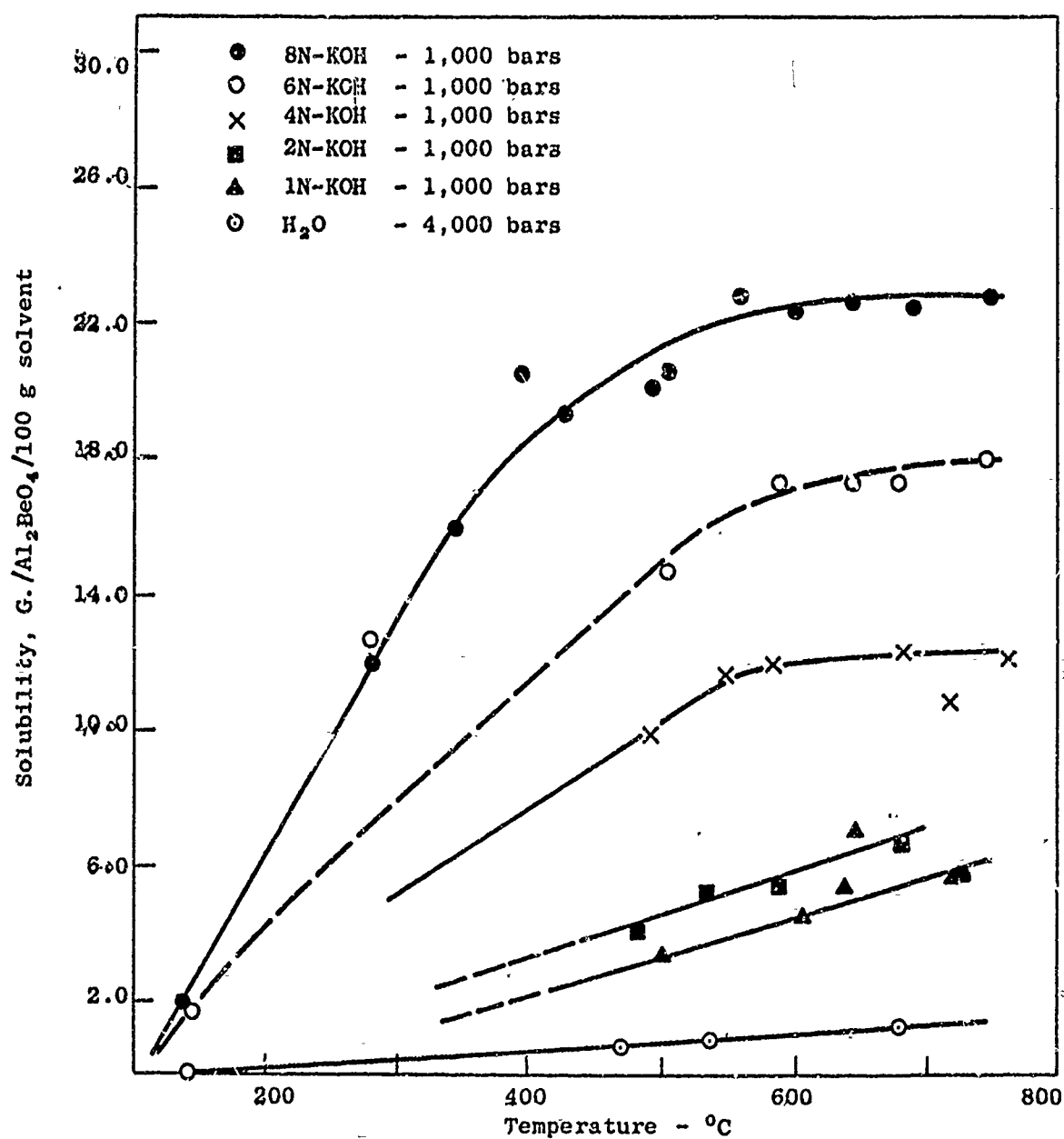


Figure 25. Solubility of Chrysoberyl in Potassium Hydroxide Solutions and Water vs Temperature at Selected Pressures.



#### IV. DISCUSSION OF RESULTS

The solubility of chrysoberyl in water at 4,000 bars was somewhat unexpected. However, its abnormally high solubility in KOH and NaOH solutions as compared to those of  $\text{Al}_2\text{O}_3$  and BeO under similar conditions follows a similar trend to the melting points of these three phases, showing that the bonds of the double oxide chrysoberyl are weaker than those of the two component oxides.

Crystals of another phase were obtained in runs with 8N-KOH and 6N-KOH, particularly in the higher temperature part of the curve. The change in slope of the solubility curves in 4 to 8N-KOH solutions with increasing temperature does suggest the presence of a reaction between KOH and chrysoberyl. Figure 26 also shows the dependence of solubility on the concentration of the KOH solution used. These observations suggest that the more dilute solutions, which have adequate solubility for chrysoberyl, may be the best solvents for growing this mineral hydrothermally.

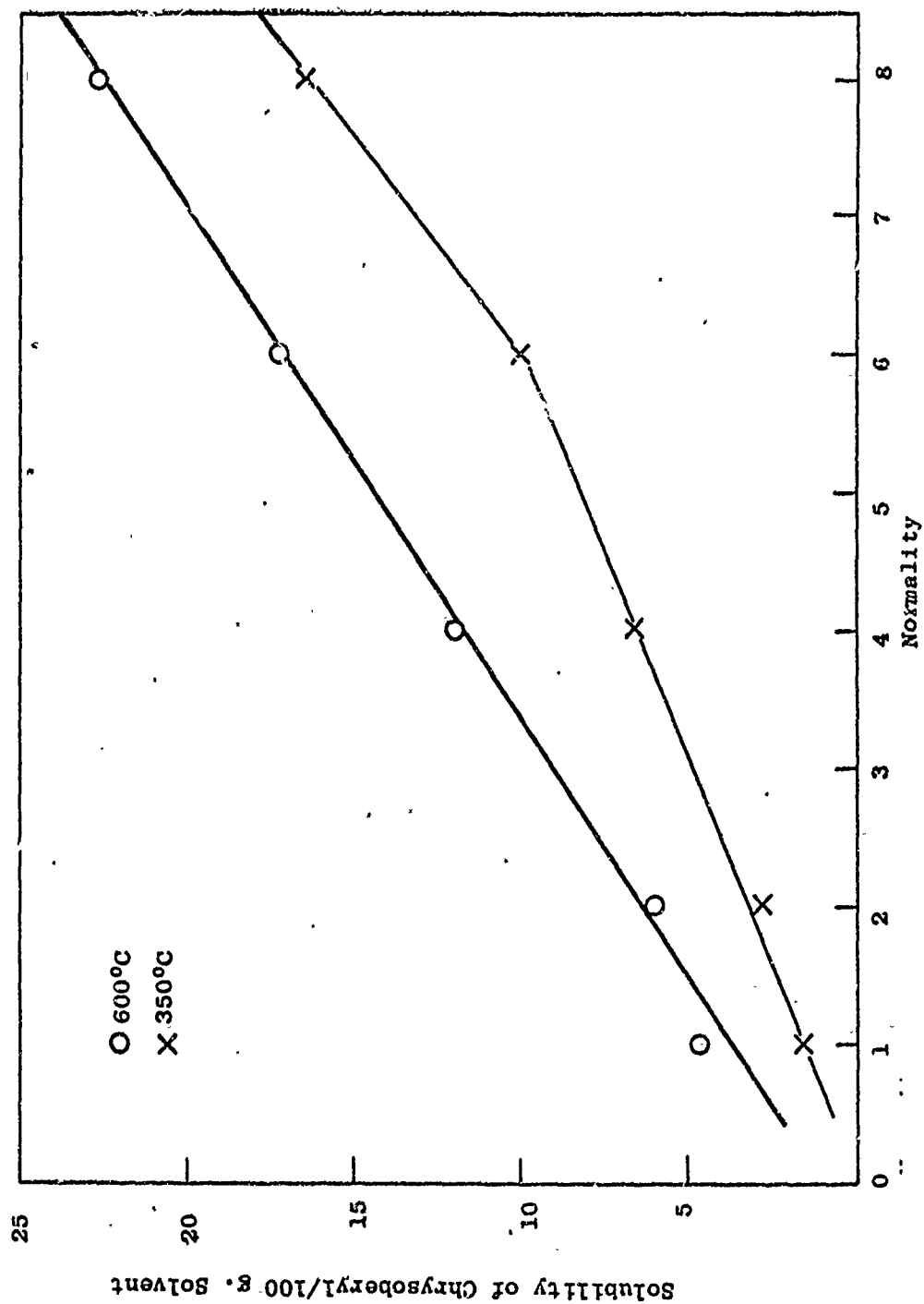


Figure 26. Solubility of Chrysoberyl in Potassium Hydroxide Solutions vs Normality at Selected Temperatures, and pressure up to 4,000 bars.

## V. REFERENCES

1. H. von Wartenberg, and H. J. Reusch; Melting Diagrams of Refractory Oxides: IV Aluminum Oxide; Z. anorg-allgem. Chem., Vol. 207, (1932). pp. 1-20.
2. R. F. Geller, P. J. Yavorsky, B. L. Steierman, and A. S. Creamer; Studies of Binary and Ternary Combinations of Magnesia, Calcia, Baria, Beryllia, Alumina, Thoria, and Zirconia in Relation to Their Use as Porcelains; J. Res. N. B. S., Vol. 36, (1946), pp. 277-312.
3. W. R. Foster and H. F. Royal; An Intermediate Compound in the System  $\text{BeO-Al}_2\text{O}_3\text{-Al}_2\text{O}_3$ , J. Am. Ceram. Soc., Vol. 32, (1949), pp. 26-34.
4. S. M. Lang, C. F. Filmore, and L. H. Maxwell; The System Beryllia-Alumina-Titania, Phase Relations and General Physical Properties of Three Components Porcelains; J. Res. N. B. S., Vol. 48, (1952), pp. 298-312.
5. F. Ya. Galakhov; Alumina Region of the Ternary Alumina-Silicate Systems, II. System  $\text{BeO-Al}_2\text{O}_3\text{-SiO}_2$ ; Izvest. Akad Nauk SSSR, Otdel. Khim. Nauk (1957), pp. 1032-1036. Chem. Abstr., Vol. 52, 6999 h (1958).
6. Charles Palache, Harry Berman and Clifford Frondell, Dana's System of Mineralogy, Vol. 1, 7th Ed., John Wiley and Sons Inc., N. Y. (1944) pp. 718-22.
7. E. F. Farrell and J. H. Fang; Flux Growth of Chrysoberyl and Alexandrite; J. Am. Ceram. Soc., Vol. 47, (1964); pp. 274-276.
8. V. G. Hill and R. I. Harker; Development of Hydrothermal Method for Growing Single Crystals of High Purity Beryllium Oxide and Lead Metaniobate; Tech. Rep. No. AFML-TR-65-297 (1965).

TABLE 7  
SUMMARY OF HYDROTHERMAL RUNS IN THE SYSTEM  $\text{KNO}_3\text{-KTAO}_3$

Run No.	Charge (% $\text{KTAO}_3$ )	Solvent	Temperature ( $^{\circ}\text{C}$ )	Pressure (bars)	Duration	Results
916	75	4N-KOH	469	4,000	19 days	Isotropic and anisotropic phases with cubic outlines. Two phases often intergrown. Xls pale blue.
901	75	8M-KOH	487	1,000	30 days	Small isotropic and anisotropic xls.
904	75	12.7M-KOH	515	1,000	4 days	Recrystallization to pale blue xls started - anisotropic.
917	75	4M-KOH	540	4,000	19 days	Isotropic and anisotropic phases often intergrown. Xls pale blue.
902	75	8M-KOH	564	1,000	30 days	Small crystals mostly isotropic, few anisotropic.
905	75	12.8M-KOH	567	1,000	4 days	Few well formed anisotropic xls.
918	75	4M-KOH	595	4,000	19 days	Mass of anisotropic xls, 0.1-0.15 mm.
903	75	8M-KOH	610	1,000	30 days	Single phase, well formed xls with cubic outline but some laths.
906	75	13.2M-KOH	610	1,000	4 days	Isotropic xls, few but well formed.
911	75	8M-KOH	643	1,000	31 days	Few xls, very fine grained.
928	75	8M-KOH	692	1,000	18 days	Isotropic xls - well formed some brown, others colorless.

Run No.	Charge (% $\text{KTaO}_3$ )	Solvent	Temperature ( $^{\circ}\text{C}$ )	Pressure (bars)	Duration	Results
912	75	8M-KOH	609	1,000	31 days	Single phase, but very fine grained.
934	75	8N-KOH	725	1,000	17 days	Principally isotropic xls. Pale blue, but with striations parallel to one axis.
1025	75	8M-KOH	789	600	16 hrs.	Cubic $\text{KTaO}_3$ SS
1035	75	8M-KOH	787	600	16 hrs.	Cubic $\text{KTaO}_3$ SS
1034	65	8M-KOH	798	600	16 hrs.	$\text{KNbO}_3$ SS + cubic $\text{KTaO}_3$ SS
1024	65	8M-KOH	801	600	16 hrs.	$\text{KNbO}_3$ SS + cubic $\text{KTaO}_3$ SS
927	65	8M-KOH	803	1,000	4 days	Two phases - isotropic and anisotropic platy habit and needles.
832	65	8M-KOH	834	1,000	3 days	Xls mostly anisotropic. Absence of striation lines parallel to growth direction.
935	65	4N-KOH	891	1,000	0.25 days	Almost completely cubic with few anisotropic xls - pale blue.
943	65	8N-KOH	1005	1,000	0.5 days	Mainly isotropic, but with some anisotropic, xls. Colorless but with evidence of exsolution along cleavage.
1023	40	8M-KOH	799	600	16 hrs.	$\text{KNbO}_3$ SS + Cubic $\text{KTaO}_3$ SS

Run No.	Charge (% $\text{KTaO}_3$ )	Solvent	Temperature ( $^{\circ}\text{C}$ )	Pressure (bars)	Duration	Results
1033	40	8M-KOH	796	600	16 hrs.	$\text{KNbO}_3$ SS + Cubic $\text{KTaO}_3$ SS
1039	40	8M-KOH	412	4,000	7 days	$\text{KNbO}_3$ SS + Cubic $\text{KTaO}_3$ SS
1040	40	8M-KOH	449	4,000	7 days	$\text{KNbO}_3$ SS + Cubic $\text{KTaO}_3$ SS
1041	40	8M-KOH	479	4,000	7 days	$\text{KNbO}_3$ SS + Cubic $\text{KTaO}_3$ SS
1028	30	8M-KOH	479	600	7 days	$\text{KNbO}_3$ SS + Cubic $\text{KTaO}_3$ SS
1022	30	8M-KOH	784	600	16 hrs.	$\text{KNbO}_3$ SS + Cubic $\text{KTaO}_3$ SS
1032	30	8M-KOH	788	600	16 hrs.	$\text{KNbO}_3$ SS + Cubic $\text{KTaO}_3$ SS
1027	20	8M-KOH	479	600	7 days	$\text{KNbO}_3$ SS + Cubic $\text{KTaO}_3$ SS
1021	20	8M-KOH	775	600	16 hrs.	$\text{KNbO}_3$ SS + Cubic $\text{KTaO}_3$ SS
1031	20	8M-KOH	793	600	16 hrs.	$\text{KNbO}_3$ SS + Cubic $\text{KTaO}_3$ SS
1026	10	8M-KOH	479	600	7 days	$\text{KNbO}_3$ SS + Cubic $\text{KTaO}_3$ SS
1042	10	8M-KOH	481	4,000	7 days	$\text{KNbO}_3$ SS + Cubic $\text{KTaO}_3$ SS
1043	10	8M-KOH	490	4,000	7 days	$\text{KNbO}_3$ SS + Cubic $\text{KTaO}_3$ SS
1020	10	8M-KOH	795	600	16 hrs.	$\text{KNbO}_3$ SS + Cubic $\text{KTaO}_3$ SS
1030	10	8M-KOH	806	600	16 hrs.	$\text{KNbO}_3$ SS + Cubic $\text{KTaO}_3$ SS
1019	0	8M-KOH	788	600	16 hrs.	$\text{KNbO}_3$

Run No.	Charge (% $\text{KTaO}_3$ )	Solvent	Temperature ( $^{\circ}\text{C}$ )	Pressure (bars)	Duration	Results
1029	0	BM-KOH	739	600	16 hrs.	$\text{KNbO}_3$

Abbreviation: Xls and xls = crystals.  
SS = solid solution

TABLE 8

SUMMARY OF DRY RUNS IN THE SYSTEM  $\text{KNbO}_3$ - $\text{KTaO}_3$ 

Charge (% $\text{KTaO}_3$ )	Temperature $^{\circ}\text{C}$	Time	Products
0	700	5 dys	$\text{KNbO}_3$
10	700	5 dys	$\text{KNbO}_3$ SS + Cubic $\text{KTaO}_3$ SS
20	700	5 dys	$\text{KNbO}_3$ SS + Cubic $\text{KTaO}_3$ SS
30	700	5 dys	$\text{KNbO}_3$ SS + Cubic $\text{KTaO}_3$ SS
40	700	5 dys	$\text{KNbO}_3$ SS + Cubic $\text{KTaO}_3$ SS
50	700	5 dys	$\text{KNbO}_3$ SS + Cubic $\text{KTaO}_3$ SS
60	700	5 dys	$\text{KNbO}_3$ SS + Cubic $\text{KTaO}_3$ SS
65	700	5 dys	$\text{KNbO}_3$ SS + Cubic $\text{KTaO}_3$ SS
75	700	5 dys	$\text{KNbO}_3$ SS + Cubic $\text{KTaO}_3$ SS
100	700	5 dys	$\text{KNbO}_3$ SS + Cubic $\text{KTaO}_3$ SS
10	800	3 dys	$\text{KNbO}_3$ SS + Cubic $\text{KTaO}_3$ SS
20	800	3 dys	$\text{KNbO}_3$ SS + Cubic $\text{KTaO}_3$ SS
30	800	3 dys	$\text{KNbO}_3$ SS + Cubic $\text{KTaO}_3$ SS
40	800	3 dys	$\text{KNbO}_3$ SS + Cubic $\text{KTaO}_3$ SS
5	1000	2 dys	$\text{KNbO}_3$ SS + Cubic $\text{KTaO}_3$ SS
10	1000	2 dys	$\text{KNbO}_3$ SS + Cubic $\text{KTaO}_3$ SS
20	1000	2 dys	$\text{KNbO}_3$ SS + Cubic $\text{KTaO}_3$ SS
30	1000	2 dys	$\text{KNbO}_3$ SS + Cubic $\text{KTaO}_3$ SS
40	1000	2 dys	$\text{KNbO}_3$ SS + Cubic $\text{KTaO}_3$ SS
50	1000	2 dys	$\text{KNbO}_3$ SS + Cubic $\text{KTaO}_3$ SS
60	1000	2 dys	Cubic $\text{KTaO}_3$ SS
65	1000	2 dys	Cubic $\text{KTaO}_3$ SS
75	1000	2 dys	Cubic $\text{KTaO}_3$ SS



TABLE 9

## SOLUBILITY DETERMINATIONS OF CHRYSOBERYL

No	Solvent	Temperature	Pressure	Duration Hours	Solubility
933	8N-KOH	750	1000 bars	14	22.9 g/100 ml.
979		680	1000	24	22.5
985		644	1000	43	22.7
984		600	1000	43	22.5
1003		558	1000	72	22.9
983		503	1000	19	20.6
1002		492	1000	72	20.2
1015		425	1000	96	19.4
1014		398	1000	96	20.6
1013		344	1000	96	16.0
1007		280	1000	144	12.0
		140	-	336	2.0
987	6N-KOH	745	1000	19	18.1
986		686	1000	19	17.5
891		645	1000	30	17.6
890		587	1000	30	17.5
889		508	1000	30	14.7
1006		280	1000	144	12.7
		140	-	336	1.9
1066	4N-KOH	769	1000	23	11.1
1062		716	1000	47	10.6
1061		682	1000	47	11.3
1065		589	1000	47	11.8
1064		550	1000	47	11.8
1063		493	1000	47	10.1
993	8N-NaOH	756	1000	72	32.9 g/100 g. solvent
997		695	1000	72	31.7
996		643	1000	72	32.6
995		592	1000	72	23.4
994		500	1000	72	22.1
1009		280	1000	144	14.8
1008	6N-NaOH	280	1000	144	12.3
		140	-	336	1.9
1018	H <sub>2</sub> O	575	4000	96	1.3
1017		536	4000	96	1.0
1016		468	4000	96	0.8
		140	-	336	0

LINED REACTOR  
WITH MODIFIED BRIDGMAN CLOSURE

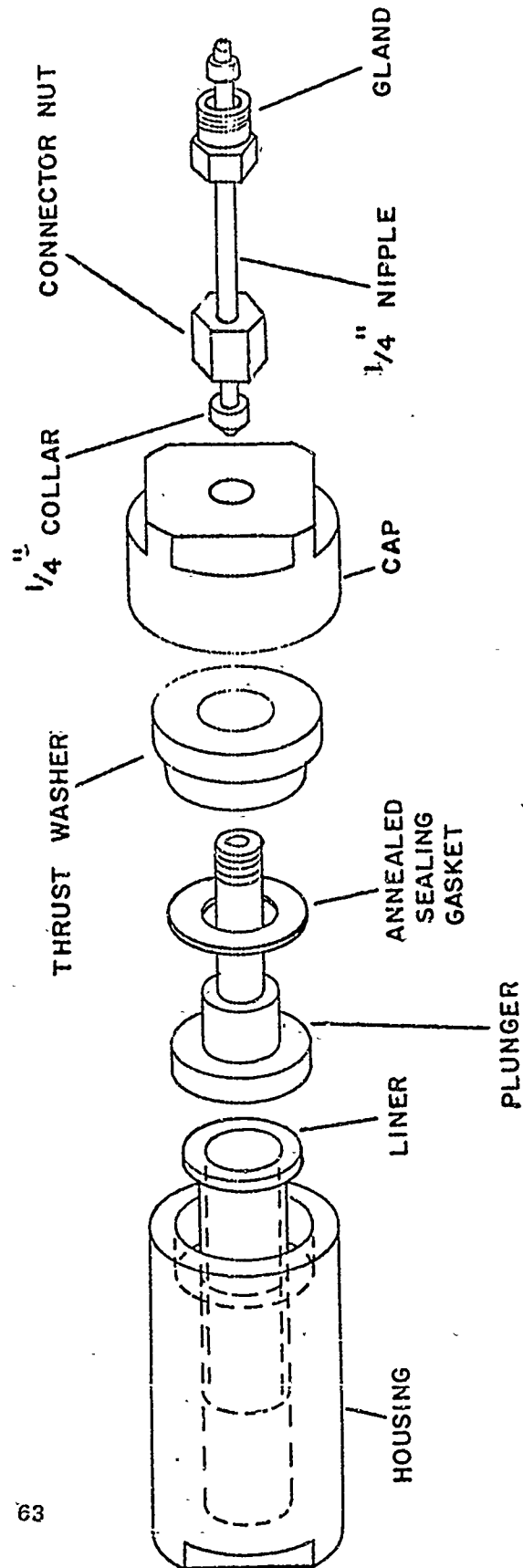


Figure 27. LRA-150 Pressure Vessel Assembly

UNCLASSIFIED

Security Classification

DOCUMENT CONTROL DATA - R&D		
(Security classification of title, body of abstract and indexing annotation must be entered when the overall report is classified)		
1. ORIGINATING ACTIVITY (Corporate author)		2a. REPORT SECURITY CLASSIFICATION
Tem-Press Research, Inc. State College, Pa. 14801		UNCLASSIFIED
		2b. GROUP
3. REPORT TITLE "Development of Hydrothermal Method for Growing Large, High Purity Single Crystals of Beryllium Oxide, and Initiate Research on Growing Single Crystals of 'KTN' and Chrysoberyl."		
4. DESCRIPTIVE NOTES (Type of report and inclusive dates)		
Technical Report - 1 Sept. 65 - 31 Aug 66		
5. AUTHOR(S) (Last name, first name, initial)		
Hill, V.G. Harker, R.I.		
6. REPORT DATE	7a. TOTAL NO. OF PAGES	7b. NO. OF REFS
October 1966	63	26
8a. CONTRACT OR GRANT NO.	9a. ORIGINATOR'S REPORT NUMBER(S)	
AF 33(615)-1712	AFML-TR-66-343	
b. PROJECT NO. 7371		
c. Task No. 737101		
d.	9b. OTHER REPORT NO(S) (Any other numbers that may be assigned this report)	
	None	
10. AVAILABILITY/LIMITATION NOTICES This document is subject to special export controls and each transmittal to foreign governments or foreign nationals may be made only with prior approval of the Air Force Materials Lab., (MAYT), Wright-Patterson Air Force Base, Ohio 45433.		
11. SUPPLEMENTARY NOTES		12. SPONSORING MILITARY ACTIVITY
		Air Force Materials Laboratory Materials Physics Division (MAYT) Wright-Patterson AFB, Ohio 45433
13. ABSTRACT		
<p>Beryllium oxide crystals weighing up to 1.07 grams have been grown hydrothermally with the nutrient temperature at <math>535 \pm 5^\circ\text{C}</math> and the growth temperature at <math>505 \pm 5^\circ\text{C}</math>. Four normal potassium hydroxide was used as hydrothermal solution. Growth occurred in the vapor phase above the potassium hydroxide solution. The quality of the seeds used has a major effect on the quality of the crystals grown. The relative growth rates in the various directions are:</p> $[11.0] > [00.1] \approx [00.1] > [11.1] > [10.1] > [10.0]$ <p>It is the positive pyramidal termination which is nucleated and grows on the seed. The crystals grown have been characterized by chemical, petrographic, and x-ray diffraction methods, and one crystal in particular has been shown to be of high quality. Growth rate measurements of BeO are reported.</p> <p>An ex-solution dome has been found in the system <math>\text{KNbO}_3\text{-KTaO}_3</math>, and the composition <math>\text{KTa}_{0.65}\text{Nb}_{0.35}\text{O}_3</math> (KTN), which has useful electro-optical properties at room temperatures, is metastable at temperatures below <math>900 \pm 10^\circ\text{C}</math>. The hydrothermal growth of KTN single crystals is, therefore, not feasible with the equipment currently available.</p> <p>Solubility determinations of chrysoberyl have been made in KOH, NaOH and water. The values obtained are far greater than those of either <math>\text{Al}_2\text{O}_3</math> or BeO.</p>		

DD FORM 1473  
1 JAN 64

UNCLASSIFIED

Security Classification

# Security Classification

14. KEY WORDS	LINK A		LINK B		LINK C	
	ROLE	WT	ROLE	WT	ROLE	WT

## INSTRUCTIONS

1. **ORIGINATING ACTIVITY:** Enter the name and address of the contractor, subcontractor, grantee, Department of Defense activity or other organization (*corporate author*) issuing the report.

2a. **REPORT SECURITY CLASSIFICATION:** Enter the overall security classification of the report. Indicate whether "Restricted Data" is included. Marking is to be in accordance with appropriate security regulations.

2b. **GROUP:** Automatic downgrading is specified in DoD Directive 5200.10 and Armed Forces Industrial Manual. Enter the group number. Also, when applicable, show that optional markings have been used for Group 3 and Group 4 as authorized.

3. **REPORT TITLE:** Enter the complete report title in all capital letters. Titles in all cases should be unclassified. If a meaningful title cannot be selected without classification, show title classification in all capitals in parenthesis immediately following the title.

4. **DESCRIPTIVE NOTES:** If appropriate, enter the type of report, e.g., interim, progress, summary, annual, or final. Give the inclusive dates when a specific reporting period is covered.

5. **AUTHOR(S):** Enter the name(s) of author(s) as shown on or in the report. Enter last name, first name, middle initial. If military, show rank and branch of service. The name of the principal author is an absolute minimum requirement.

6. **REPORT DATE:** Enter the date of the report as day, month, year, or month, year. If more than one date appears on the report, use date of publication.

7a. **TOTAL NUMBER OF PAGES:** The total page count should follow normal pagination procedures, i.e., enter the number of pages containing information.

7b. **NUMBER OF REFERENCES:** Enter the total number of references cited in the report.

8a. **CONTRACT OR GRANT NUMBER:** If appropriate, enter the applicable number of the contract or grant under which the report was written.

8b, 8c, & 8d. **PROJECT NUMBER:** Enter the appropriate military department identification, such as project number, subproject number, system numbers, task number, etc.

9a. **ORIGINATOR'S REPORT NUMBER(S):** Enter the official report number by which the document will be identified and controlled by the originating activity. This number must be unique to this report.

9b. **OTHER REPORT NUMBER(S):** If the report has been assigned any other report numbers (either by the originator or by the sponsor), also enter this number(s).

10. **AVAILABILITY/LIMITATION NOTICES:** Enter any limitations on further dissemination of the report, other than those

imposed by security classification, using standard statements such as:

- (1) "Qualified requesters may obtain copies of this report from DDC."
- (2) "Foreign announcement and dissemination of this report by DDC is not authorized."
- (3) "U. S. Government agencies may obtain copies of this report directly from DDC. Other qualified DDC users shall request through \_\_\_\_\_."
- (4) "U. S. military agencies may obtain copies of this report directly from DDC. Other qualified users shall request through \_\_\_\_\_."
- (5) "All distribution of this report is controlled. Qualified DDC users shall request through \_\_\_\_\_."

If the report has been furnished to the Office of Technical Services, Department of Commerce, for sale to the public, indicate this fact and enter the price, if known.

11. **SUPPLEMENTARY NOTES:** Use for additional explanatory notes.

12. **SPONSORING MILITARY ACTIVITY:** Enter the name of the departmental project office or laboratory sponsoring (paying for) the research and development. Include address.

13. **ABSTRACT:** Enter an abstract giving a brief and factual summary of the document indicative of the report, even though it may also appear elsewhere in the body of the technical report. If additional space is required, a continuation sheet shall be attached.

It is highly desirable that the abstract of classified reports be unclassified. Each paragraph of the abstract shall end with an indication of the military security classification of the information in the paragraph, represented as (TS), (S), (C), or (U).

There is no limitation on the length of the abstract. However, the suggested length is from 150 to 225 words.

14. **KEY WORDS:** Key words are technically meaningful terms or short phrases that characterize a report and may be used as index entries for cataloging the report. Key words must be selected so that no security classification is required. Identifiers, such as equipment model designation, trade name, military project code name, geographic location, may be used as key words but will be followed by an indication of technical context. The assignment of links, rules, and weights is optional.